





Article

lncRNA–miRNA–mRNA ceRNA Network Involved in Sheep Prolificacy: An Integrated Approach

Masoumeh Sadeghi ^{1,†}, Abolfazl Bahrami ^{2,3,*,†} , Aliakbar Hasankhani ^{2,†} , Hamed Kioumarsi ⁴ ,
Reza Nouralizadeh ^{5,*}, Sarah Ali Abdulkareem ⁶, Farzad Ghafouri ² and Herman W. Barkema ⁷ 

- ¹ Environmental Health, Zahedan University of Medical Sciences, Zahedan 98, Iran; sadeghimasooome2@gmail.com
- ² Department of Animal Science, College of Agriculture and Natural Resources, University of Tehran, Karaj 31, Iran; a.hasankhani74@ut.ac.ir (A.H.); farzad.ghafouri2@ut.ac.ir (F.G.)
- ³ Biomedical Center for Systems Biology Science Munich, Ludwig-Maximilians-University, 80333 Munich, Germany
- ⁴ Department of Animal Science Research, Gilan Agricultural and Natural Resources Research and Education Center, Agricultural Research, Education and Extension Organization (AREEO), Rasht 43, Iran; hkioumars@yahoo.com
- ⁵ Department of Food and Drug Control, Faculty of Pharmacy, Jundishapur University of Medical Sciences, Ahvaz 63, Iran
- ⁶ Department of Computer Science, Al-Turath University College, Al Mansour, Baghdad 10011, Iraq; sarah.ali@turath.edu.iq
- ⁷ Department of Production Animal Health, Faculty of Veterinary Medicine, University of Calgary, Calgary, AB T2N4Z6, Canada; barkema@ucalgary.ca
- * Correspondence: a.bahrami@ut.ac.ir (A.B.); nouralizadeh.r@ajums.ac.ir (R.N.); Tel.: +98-9199300065 (A.B.)
- † These authors contributed equally to this work.



Citation: Sadeghi, M.; Bahrami, A.; Hasankhani, A.; Kioumars, H.; Nouralizadeh, R.; Abdulkareem, S.A.; Ghafouri, F.; Barkema, H.W. lncRNA–miRNA–mRNA ceRNA Network Involved in Sheep Prolificacy: An Integrated Approach. *Genes* **2022**, *13*, 1295. <https://doi.org/10.3390/genes13081295>

Academic Editors: Cord Drögemüller and Gesine Lühken

Received: 10 June 2022

Accepted: 19 July 2022

Published: 22 July 2022

Publisher's Note: MDPI stays neutral with regard to jurisdictional claims in published maps and institutional affiliations.



Copyright: © 2022 by the authors. Licensee MDPI, Basel, Switzerland. This article is an open access article distributed under the terms and conditions of the Creative Commons Attribution (CC BY) license (<https://creativecommons.org/licenses/by/4.0/>).

Abstract: Understanding the molecular pattern of fertility is considered as an important step in breeding of different species, and despite the high importance of the fertility, little success has been achieved in dissecting the interactome basis of sheep fertility. However, the complex mechanisms associated with prolificacy in sheep have not been fully understood. Therefore, this study aimed to use competitive endogenous RNA (ceRNA) networks to evaluate this trait to better understand the molecular mechanisms responsible for fertility. A competitive endogenous RNA (ceRNA) network of the corpus luteum was constructed between Romanov and Baluchi sheep breeds with either good or poor genetic merit for prolificacy using whole-transcriptome analysis. First, the main list of lncRNAs, miRNAs, and mRNA related to the corpus luteum that alter with the breed were extracted, then miRNA–mRNA and lncRNA–mRNA interactions were predicted, and the ceRNA network was constructed by integrating these interactions with the other gene regulatory networks and the protein–protein interaction (PPI). A total of 264 mRNAs, 14 lncRNAs, and 34 miRNAs were identified by combining the GO and KEGG enrichment analyses. In total, 44, 7, 7, and 6 mRNAs, lncRNAs, miRNAs, and crucial modules, respectively, were disclosed through clustering for the corpus luteum ceRNA network. All these RNAs involved in biological processes, namely proteolysis, actin cytoskeleton organization, immune system process, cell adhesion, cell differentiation, and lipid metabolic process, have an overexpression pattern (Padj < 0.01). This study increases our understanding of the contribution of different breed transcriptomes to phenotypic fertility differences and constructed a ceRNA network in sheep (*Ovis aries*) to provide insights into further research on the molecular mechanism and identify new biomarkers for genetic improvement.

Keywords: corpus luteum; RNA-seq; lncRNA–miRNA–mRNA ceRNA network; protein–protein interaction; prolificacy; sheep

1. Introduction

Enhancing fertility will improve the efficiency of animal production and reproduction. Expansion of reproductive performance will boost the lifetime of a sheep, reduce veterinary treatments and costs, lower insemination efforts, and shorten the lambing interval [1]. Fertility is a critical factor for the sustainability of sheep farming. Although, since the 1980s, fertility in sheep and cattle has reduced and has become one of the major causes for culling and replacement [2–4]. Few studies have been done in the last decades to survey the genetic bases of this decline in fertility, considering the reproduction process focusing on some particular stages of reproduction. A study has shown that reproductive traits in ewe can be regulated by individual genetic markers with major effects, known as prolificacy genes [5], or by polygenic effects, specifically in prolific sheep breeds, such as Romanov [6]. Several mutations in major genes, such as *B4GALNT2*, *BMPR1B*, *BMP15*, and *GDF9*, control litter size and ovulation rates in the ewe [7–9]. In recent years, microarray and transcriptomic analysis through RNA-seq of different ewe reproduction tissues have furnished additional understandings of the gene expression, and a few novel genes (e.g., *IL1B*, *IL1A*, *UCP2*, *STAR*, and *PTGS2*) have been discovered to be associated with fecundity in the ewe [10]. Earlier studies have demonstrated that high prolificacy can result from the action of either a single gene with a major effect, as in small-tailed Han, Lacaune, Booroola Merino, and the Chinese Hu breeds [11–13], or various sets of genes, as in the Romanov and Finnsheep breeds [14]. The Romanov, one of the most highly prolific sheep, has been exported to more than 40 countries to improve regional sheep, although the ovulation rate heritability is low [15]. Recently, a FecGF mutation in gene *GDF9* has been recognized to be strongly associated with prolificacy in Finnsheep and other breeds [16]. The success of pregnancy in ewes and other ruminants is demarcated at the preimplantation stage, in which the corpus luteum (CL) and endometrium play vital roles [17]. Therefore, applied knowledge of molecular mechanisms was expected to help in identifying hub genes or modules and explaining interactions between fertility and other traits [18]. For example, oocyte or spermatozoa quality and their interactions, as well as embryo and fetus developmental stages, have been recognized using omics tools in different species [19]. However, the significance of RNAs in sheep fertility features remained unknown.

Omics directs the usage and the high-throughput technologies' output analysis to identify and interpret the genomics, transcriptomics, proteomics, metabolomics, and epigenetics levels [20]. Further, QTL (quantitative trait loci), gene mapping, and functional genomics investigations have been carried out to explore the most important genes associated with reproductive traits [21]. Unfortunately, no clear picture has appeared at omics levels for sheep prolificacy, specifically. Accordingly, reproductive success in sheep is now seen as the result of complex interactions between different factors and omics levels [22]. On the other hand, fertility has been of high economic value in recent decades, and compared with other mammals, sheep are a potential model for studying the genetic basis of reproductive traits [23,24]. Complex interactions between the fetus, ovary, corpus luteum (CL), and endometrium are affected by maintenance and facility of pregnancy. In this regard, the endometrium stimulates embryo development through secretions in the histotroph [25–27]. After ovulation, a critical step in the rapid ascent of progesterone (P4) concentration is the cellular reorganization of the ovulatory follicle to create a highly vascularized CL [28]. The corpus luteum (CL) is an obvious target for differentially expressed genes studies to detect hub genes between low-fertility and high-fertility breeds [29]. An integrated approach is needed to decipher the large-scale data generated with high-throughput technologies. Integrated analyses can combine multilevel views of physiology data into a holistic interpretation of nonlinear molecular procedures [30,31]. Currently, large databases of big biological/computational data are available including interactions and records of protein functions. Correspondingly, various bioinformatics tools, computational approaches, and algorithms have been designed to discover key regulatory modules in the different complex biological networks [32,33]. Regardless, few components of these interactions have been studied for decades, and the accumulation of large-scale datasets to construct

networks is a unique advancement in genetics and medicine [34,35]. Moreover, the recent improvement in molecular biology data has highlighted the urgency of integrating networks such as lncRNA–miRNA–mRNA ceRNA networks. Multi-partite networks consider various RNAs and have disclosed a new mechanism of interaction between RNAs. Long non-coding RNAs (lncRNAs), a category of non-coding RNA transcripts longer than 200 nucleotides [36], are known to be involved in considerable biological procedures, such as cell proliferation and transcriptional regulation [37]. Similarly, miRNAs (micro-RNAs), a category of short non-coding RNAs, play critical regulatory roles in multiple biological procedures, such as cell differentiation, cell migration, oncogenesis, and apoptosis, by suppressing the mRNA [38]. Nonetheless, the complex mechanisms associated with prolificacy in sheep have not been fully comprehended. Interestingly, the need to use this approach to understand the molecular regulatory mechanisms behind polygenic traits and to fully dissect the etiology of complex traits becomes even more important [39,40]. Thereby, analysis of molecular pathways has the potential to illuminate the trait progression and response to treatment at the molecular level. Accordingly, the identification of hub genes, proteins, and pathways can be understood by utilizing gene/protein interaction network models.

In this study, we conducted multi-partite networks on reproductive traits, specifically litter size in the sheep breeds of high (Romanov) and low (Baluchi) fertility, with a litter size ranging from one to four, from different geographic regions of the farms, respectively. Romanov sheep show outstanding reproduction qualities: early sexual maturity, out-of-season breeding, and extraordinary fertility. However, the Baluchi sheep is a relatively low-prolificacy breed originally from Khorasan Razavi province, Iran, and excels in fleece weights and muscle growth [41]. Therefore, a comparison of the transcriptomic level by integrative analysis and the other integrated multi-omics level in these two breeds can help us to identify related genes and ncRNAs, their functions, and the important pathways for further genetic improvement of the reproduction traits in sheep as well as other mammals.

In this way, a ceRNA network consisting of lncRNA–miRNA–mRNA was constructed based on lncRNA–mRNA and miRNA–mRNA interactions. In addition, the other networks including protein–protein interaction networks (PPI), metabolic pathways, and gene regulatory networks (GRNs) of the hub genes involved in the ceRNA network were conducted to explore the effects of functional modules and hub differentially expressed genes, miRNAs, and lncRNAs on prolificacy. Overall, our results suggest a group of genes or mRNAs, miRNAs, and lncRNAs using a computational approach that can play key and potential roles in transcriptional and post-transcriptional gene regulation under different conditions.

2. Materials and Methods

The complete workflow for the sample collection, preparation, sequencing, and analysis of relevant species related to the corpus luteum in two sheep breeds is presented in Figure 1.

2.1. Sample Collection

A total of 48 ewes from two sheep breeds of high prolificacy (Romanov, $n = 24$) and one of low prolificacy (Baluchi, $n = 24$) were collected from University of Tehran scientific park in Iran. The sheep included were as unrelated as possible based on records for the phenotype of litter size and the other reproductive traits. Data for the phenotype of litter size records are presented in Supplementary Table S1.

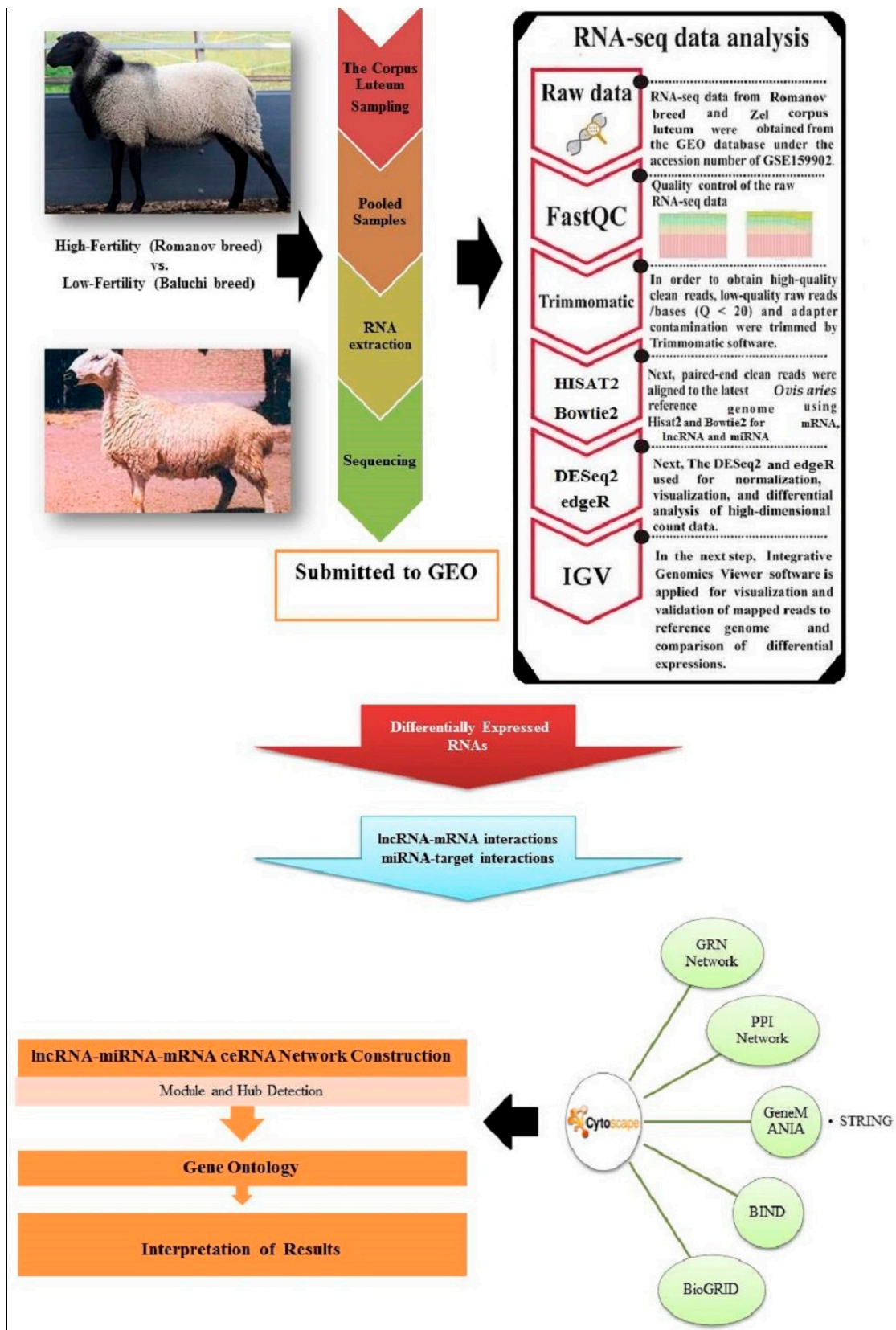


Figure 1. Schematic of the pipeline used to construct lncRNA–miRNA–mRNA ceRNA network of the corpus luteum in sheep. The main RNAs were identified from the RNA-Seq dataset between two different breeds. The protein–protein interaction network (PPI) and gene regulatory network (GRN) were constructed and visualized using Cytoscape 3.9.1.

2.2. Ovulation Synchronization

Sheep were synchronized based on a protocol (CIDR) described by Herlihy et al. [42] and CL samples were collected at appointed dates. On day -10 , each sheep was administered an i.m. injection of a gonadotropin-releasing hormone (GnRH) agonist, and an internal drug release device (CIDR; Pfizer; Germany) was inserted per vaginam. Then, on day -3 , each sheep was administered an i.m. injection of prostaglandin $F2\alpha$ (PGF 2α) (Lutalyse; Pfizer; Germany). Then, on day -2 , the CIDR device was again removed, and 24 h later, each sheep was administered a second i.m. injection of GnRH agonist.

2.3. Tissue Biopsies

On day 10 of the estrous cycle, CL biopsies were collected from each sheep as described previously [43,44]. Briefly, sheep were sedated with intravenous xylazine, and caudal epidural anesthesia was induced to prevent abdominal straining. The luteal biopsy was performed using a tissue biopsy needle (Ovum Pick-up instrument equipped with a 48 cm long trocar tip; SABD-1648-15-T; US Biopsy; Canada). In the biopsy sample, the mean luteal tissue area was 425 mm² (range, 313 to 524 mm²). Some corpora lutea contained a central luteal cavity with an area of 335 mm². A total of 59 biopsy attempts were made; 54 (92%) resulted in obtaining a luteal tissue specimen at the first attempt. The average size of the obtained biopsy core was 1 mm in diameter and 10.8 mm in length (range, 10 to 12 mm), and the average weight was 4.4 mg (range, 1.8 to 7.5 mg). CL samples were instantly frozen in liquid nitrogen and stored at -80 °C.

2.4. RNA Extraction

Whole RNA was extracted from CL (HF and LF) samples using a Trizol-based method [45]. Whole RNA was purified using the miRNeasy kit (Qiagen; Hilden, Germany) for removing any DNA contamination. The RNA quality and concentration were determined using a NanoDrop ND-1000 spectrophotometer (NanoDrop Technologies LLC; Wilmington, DE, USA). The 260/280 nm ratio of absorbance ranged from 1.85 to 2.13 for all CL samples.

2.5. cDNA Library Preparation and Sequencing

The RNA samples were converted to cDNA libraries for sequencing based on the protocol of the Illumina TruSeq RNA Sample Preparation Kit (Illumina; San Diego, CA, USA). RNA-Seq libraries were amplified by 11 cycles of PCR. Library concentration and quality were determined by Qubit (Invitrogen; Corston, UK) and Bioanalyser 2100 (Agilent Technologies; Santa Clara, CA, USA). Each sample was sequenced on a single lane over a total of two flow cells on the Illumina HiSeq 2500 platform to generate 60 million 50-base paired-end reads, and FASTQ files were created using CASAVA (v1.9) (Illumina).

2.6. Quality Assessment and Adapter Trimming of Raw Sequencing Data

A quality check of the raw sequence data was accomplished using FastQC software (v0.11.9) [46]. For this purpose, the raw RNA-seq reads were imputed into the software and the sequence quality, basic statistics, sequence content, and quality score were evaluated per base. The raw sequence data that had the needs of quality features were utilized for the next analysis. Next, PCR primers, the adapters, and non-informative sequences were trimmed using the Trimmomatic software (v0.38.1) [47].

2.7. Sequence Alignment and Detection of RNAs

Alignment sequences, mapping, and identification of known and novel RNAs of reads were conducted on the Ovis aries reference genome (http://ftp.ensembl.org/pub/release-103/fasta/ovis_aries/dna/ (accessed on 29 December 2020)) using HISAT2 software (v2.2.1) [48].

2.8. Analyzing Differentially Expressed RNAs

For transcript quantification, featureCounts software (v2.0.1) was utilized to calculate the total raw counts of mapped reads [49]. Next, to examine whether the accumulation or degradation of transcripts was related to prolificacy, the transcripts and their expression levels were compared between corpus luteum samples of Romanov and Baluchi sheep. Differentially expressed transcripts (DETs) were performed from reading counts using DESeq2 software (v2.11.40.7) [50]. For this step, normalization of the data was performed in such a way that the raw read count of each transcript was multiplied by the sample size factor, which was calculated as a ratio of the observed count. For each transcript in each corpus luteum sample, the observed count is the ratio of the raw count for each transcript to the geometric mean across the samples. At the end of the analysis, transcripts with a false discovery rate (FDR) <0.05 and log₂ fold change difference data were performed, and those with *inadj* <0.01 were considered as differentially expressed mRNAs and lncRNAs. For miRNA identification, quality control was performed using FastQC with default parameters. Clean tags were obtained by removing low-quality reads. Meanwhile, the clean tags were mapped to the reference genome using Bowtie2 [51]. The mapping percentage ranged from 66.45% to 80.02%, with an average of 76.74%. Differentially expressed miRNAs were identified using the generalized linear model implemented in edgeR [52] software, with thresholds FDR < 0.05 and fold-change difference ranging from 66.45% to 80.02%, with an average of 76. For the Seq results, an IGV 2.3 (Integrative Genomics Viewer) tool was used [53].

2.9. Validation of RNA-Seq Results Using Quantitative Real-Time PCR

To validate the reproducibility of RNA-seq data, four DEGs including *BMP2*, *HNF4A*, *PLCB2*, and *RPS6KL1* were selected for analysis by qRT-PCR. The same RNAs extracted from the CL tissues at each breed were used for qRT-PCR validation. The primer pairs were designed using Geneious Prime software v2021.1 (Supplementary Table S2). Quantitative reverse-transcription PCR was carried out according to the manufacturer's specifications for reference to SYBR[®] Premix Ex Taq[™]. SYBR Green PCR cycling was denatured using a program of 95 °C for 10 s, and 35 cycles of 95 °C for 5 s, and 60 °C for 40 s, and performed on an ABI 7500 instrument (USA). The specificity of each PCR product was confirmed by melting curve analysis. All qRT-PCR assays were performed in triplicate reactions. The housekeeping genes *RPL19* and *GAPDH* (glyceraldehyde-3-phosphate dehydrogenase) were used as the internal control genes. The expression levels of target mRNAs were obtained based on RNAs extracted from the four ewes and were shown to be normalized to *GAPDH*.

2.10. Gene Annotation

Gene set annotation enrichment analysis was also carried out using the online programs g: Profiler [54] (<https://biit.cs.ut.ee/gprofiler/gost> (accessed on 12 March 2022)), GeneCards (www.genecards.org/ (accessed on 12 March 2022)), the STRING database [55] (<https://string-db.org> (accessed on 12 March 2022)), and the DAVID [56] (Database for Annotation, Visualization, and Integrated Discovery; <https://david.ncifcrf.gov/> (accessed on 12 March 2022)), which provide a set of functional annotation tools for the genes categorized using gene ontology (GO) terms.

2.11. Target Prediction and Validation of Differentially Expressed mRNAs, lncRNAs, and miRNAs

The predicted and validated mRNA genes were identified using miRWalk 3.0 (<http://129.206.7.150/> (accessed on 23 December 2021)), a comprehensive atlas of microRNA–target interaction tools, which integrates 12 miRNA–target prediction tools. Further, lncRNA–mRNA interactions were predicted by the NONCODE database [57] (<http://www.noncode.org/> (accessed on 3 January 2021)) and the LNCipedia database [58] (<https://lncipedia.org> (accessed on 3 January 2021)).

2.12. lncRNA–miRNA–mRNA ceRNA Network Construction and Gene Ontology

lncRNA–miRNA–mRNA ceRNA network was constructed based on miRNA–mRNA and lncRNA–mRNA interactions and online interaction databases. The Pathway Resource List (<http://pathguide.org> (accessed on 15 March 2022)) is a meta-database that provides more than 300 web-accessible network databases and biological pathways [59]. PPI (protein–protein interaction) data were abstracted from the Database of Interacting Proteins [60], BIND (Biomolecular Interaction Network Database) [60], MIPS (Mammalian Protein–Protein Interactions Database) [61], and BioGRID (Biological General Repository for Interaction Datasets) [62]. In addition, interaction data were obtained from the analysis of related experiments and search in interaction databases such as Gene-MANIA [63] (<https://genemania.org/> (accessed on 15 March 2022)) and the STRING database [64] (Search Tool for the Retrieval of Interacting Genes or Proteins; <https://string-db.org> (accessed on 15 March 2022)). To describe the interaction between proteins using a probabilistic confidence score, the string uses eight major sources of interaction or association data, including co-occurrence, neighborhood, fusion, co-expression, experimental, text mining, and database [64].

Moreover, several Cytoscape plugins were used for different purposes such as screening, integrating, visualizing, and analyzing interactive data. In the respective networks, molecular species (RNAs) and the interactions between them are represented as nodes and edges, respectively. Gene Ontology terms with FDR < 0.05 were considered significantly enriched for the identified genes. Furthermore, constructed networks were compiled in simple interaction format (SIF) bowed to Cytoscape for topological analysis. Then, the statistical and topological significance of the network was assessed using the Network Analyzer plugin in Cytoscape software (v3.8.2.) [1] (National Institute of General Medical Sciences, Bethesda Softworks, Rockville, MD, USA). The mean path length, the degree of nodes, the network diameter, and the shortest path lengths between any two nodes compared with random networks (Barabasi–Albert and Erdos–Renyi models) were analyzed.

2.13. Clustering of lncRNA–miRNA–mRNA ceRNA Network

Topological properties of the lncRNA–miRNA–mRNA ceRNA network were evaluated by Cytoscape software (v3.8.2.) and, for clustering, ClusterONE [65] and MCODE [66] were used. ClusterONE was developed to discover densely connected sub-graphs of a network by minimizing edges between different clusters and maximizing edges within a cluster. MCODE is a clustering algorithm, which can be used for directed or undirected graphs.

3. Results

3.1. Candidate lncRNA, miRNA, and mRNA/Gene List

A summary of the RNA-seq data analysis pipeline and the steps of constructing of lncRNA–miRNA–mRNA ceRNA network is shown in Figure 1. A total of 264 genes/mRNAs, 14 lncRNAs, and 34 miRNAs in the corpus luteum samples of Romanov compared with Baluchi sheep were identified from RNA-Seq data. The total RNAs in these two breeds that are known to be involved in prolificacy are given in Supplementary Table S3. These RNAs are annotated and described based on the molecular and biological processes in the Gene Ontology (GO) databases. For validation of alignment related to transcripts, the result of aligned reads corresponding to one of the key genes of interest (AGR2) is shown in Figure S1.

3.2. Global Transcriptome Was Differentially Expressed in Romanov Compared with Baluchi Sheep

To discover the prolificacy of the mRNA–lncRNA–miRNA regulatory network, we first analyzed the global transcriptome in CL in both Romanov and Baluchi sheep breeds. Using the hierarchical clustering algorithm, we detected that the global gene expression is changed in CL (Supplementary Table S4), with 155 and 3 mRNAs/genes and lncRNAs significantly up-regulated (FDR < 0.05, fold-change > 1.5) and 109 and 11 mRNAs/genes and lncRNAs significantly down-regulated (FDR < 0.05, fold-change < –1.5), respectively. We identified a total of 34 miRNAs altogether. Moreover, we identified 19 up-regulated

and 15 down-regulated miRNAs by comparing the gene expression profile of Romanov with Baluchi through applying stringent filtering criteria (false discover rate, FDR < 0.05, fold-change > 1.5, and $p < 0.01$) (Supplementary Table S5).

3.3. Analysis of Expression based on RT-qPCR Data

To assess the accuracy and reliability of differentially expressed genes identified by RNA-seq, four DEGs from two breeds were selected to perform qRT-PCR tests. The expression results for four genes assessed using RNA-seq and qRT-PCR are shown in Figure 2. As can be observed, the expression patterns of four genes showed a general agreement between the two technologies.

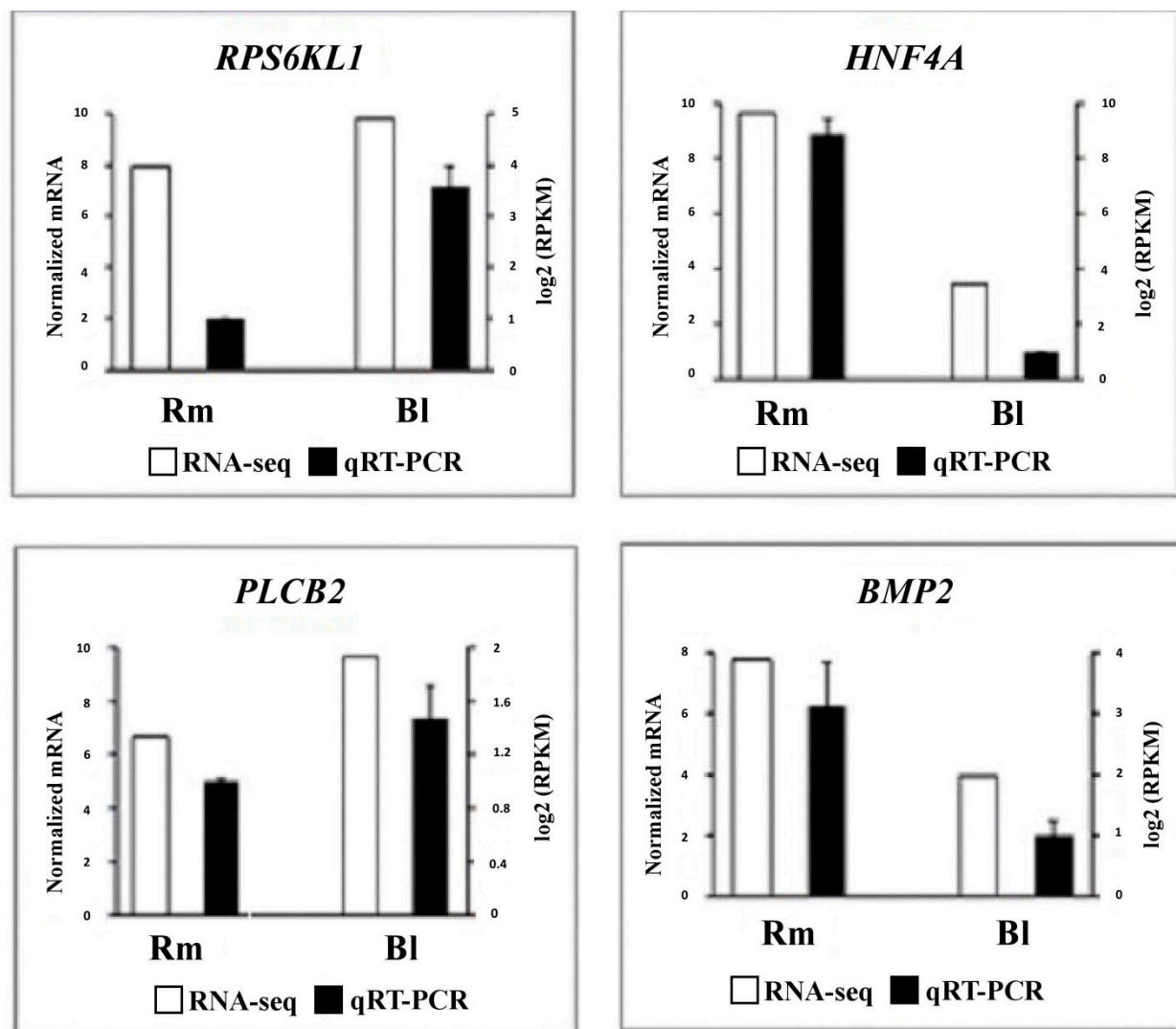


Figure 2. Differentially expressed genes were selected from transcriptome comparison combinations at different breeds. The black-filled columns represent the relative mRNA expression levels obtained by qRT-PCR, which were normalized by GAPDH; the blank columns show the log₁₀ (RPKM) value obtained by RNA-seq. Rm and Bl represent Romanov and Baluchi breeds, respectively.

3.4. GO and Pathway Analysis of Differentially Expressed mRNAs

GO analysis was used to explore the function of the significantly altered mRNAs/genes. The differentially expressed mRNAs were mainly enriched in six molecular function terms containing proteolysis, actin cytoskeleton organization, immune system process, biological adhesion, cell differentiation, and the lipid metabolic process. The KEGG, WikiPathways, and Reactome analysis was performed to identify pathways that were significantly en-

riched with differentially expressed mRNAs ($p < 0.05$) (Figure 3A). Among these pathways, the Wnt signaling pathway contained the largest number of differentially expressed genes.

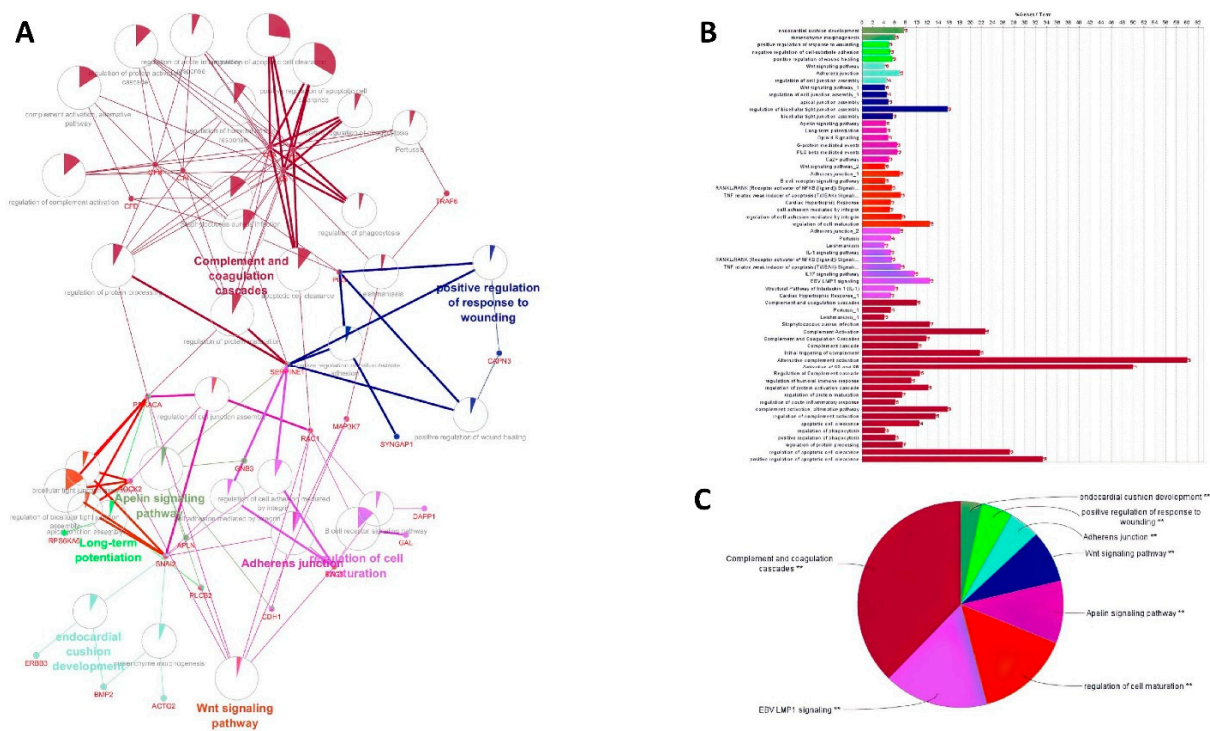


Figure 3. (A) Gene Ontology was constructed by integrating KEGG, Reactions, and WikiPathways. Each node illustrates a pathway or term and the percentage of visible shared genes between pathways or terms and edges present relationships between pathways; (B) bar chart shows the number of genes and related pathways using ClueGO and CluePrdia software based on different databases (C) pie chart shows the number of genes and related pathways using ClueGO and CluePrdia software based on different databases. ** represents hub genes were significantly enriched in these biological processes and molecular functions.

3.5. Construction of lncRNA–miRNA–mRNA ceRNA Network

To discover the mechanism of how lncRNAs regulate mRNA through sponging miRNA, a ceRNA network was constructed with a combination of predicted miRNA–mRNA and lncRNA–mRNA interactions. Based on the knowledge of interactions in databases, we could detect interactions for 312 nodes and 748 edges in the network. Moreover, the related files of networks are given in Supplementary Table S6. Finally, 264 differentially expressed mRNAs, 14 differentially expressed lncRNAs, and 34 differentially expressed miRNAs were included in the network. To further explore the most significant clusters of mRNAs/genes in the ceRNA network, we conducted PPI network, BIND, MIPS, and BioGRID. In addition, interaction data were extracted from the analysis of related experiments and search in interaction databases such as GeneMANIA and the STRING database. As mentioned, molecular species (mRNAs, lncRNAs, and miRNAs) in constructed networks are indicated as nodes and the interactions between them as edges. Moreover, constructed networks were compiled in simple interaction format (SIF) bowed to Cytoscape (v3.8.2.) (National Institute of General Medical Sciences, Bethesda Softworks, Rockville, MD, USA) for topological analysis.

3.6. Topology Analysis

Network characteristics were calculated using the Network Analyzer plugin of Cytoscape for the ceRNA Network. Topological analysis recognizes the qualitative virtues of the complex biological systems. Network topology is used to examine the state of communication and information transfer of a node with other nodes of interactive networks.

Topological parameters such as the average clustering coefficient of degrees, topological coefficient, average degree, betweenness centrality, and power-law distribution were evaluated. The distribution of the clustering coefficient is an important parcel of biological scale-free networks. Then, network density, characteristic path length, network centralization, and the clustering coefficient of the ceRNA network were compared with randomized model networks (Barabasi–Albert and Erdos–Renyi models), as presented in Table 1. The structure of the ceRNA network is far from the structure of the simulated randomized network. In particular, the clustering coefficient of the ceRNA network is significantly different from the random network.

Table 1. Basic network statistics of the two generated networks, compared with simulated randomized model networks.

	lncRNA–miRNA–mRNA ceRNA Network	Simulated Barabasi Albert Model (Scale Free)	Simulated Erdos–Renyi Model
Number of nodes	312	312	312
Clustering coefficient	0.108	0.006	0.004
Characteristic path length	4.192	4.947	4.432
Network density	0.006	0.007	0.007
Network centralization	0.070	0.012	0.009

3.7. Clustering of lncRNA–miRNA–mRNA ceRNA Network

Finally, we utilized clustering on the lncRNA–miRNA–mRNA ceRNA network made by an integrated approach. Clustering algorithms are utilized to determine significant sub-networks or modules. The results were clustered by ClusterONE [65] and MCODE software [66]. ClusterONE output was 19 modules or clusters including 68 nodes. MCODE output was 13 modules including 89 nodes (considering overlapping cluster nodes). Some of the clusters turned out to be sub-clusters of other larger clusters, so such sub-clusters were removed and the final number of clusters was diminished from 13 to 6 modules. Many of the nodes are repeated in more than one cluster and, in total, there were 44, 7, and 7 unique mRNAs/genes, lncRNAs, and miRNAs, respectively, out of six modules (Figures 4–9). These clusters are shown in Supplementary Table S7. For constructing a pathway network, different databases were integrated and percentages of visible nodes at each term are shown in Figure 4.

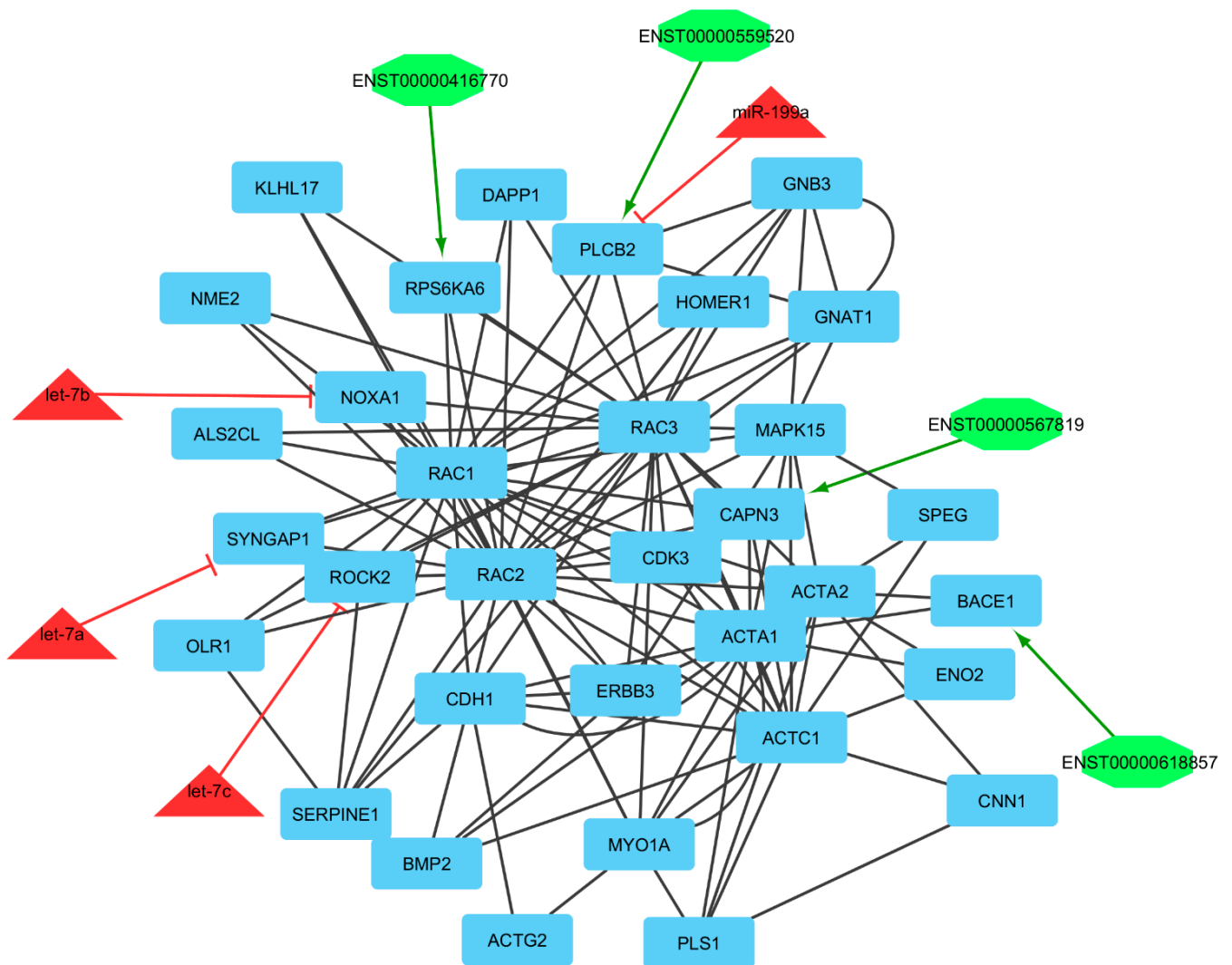


Figure 4. Module 1: 33 mRNAs/genes, 4 lncRNAs, and 4 miRNAs in an interacted network were identified. In this network, the quadrilateral nodes represent mRNAs/genes, octagonal nodes represent lncRNAs, and triangle nodes represent miRNAs. Edges indicate the interactions; black edges represent mRNA–mRNA interactions, green edges represent lncRNA–mRNA interactions, and red edges represent miRNA–mRNA interactions.

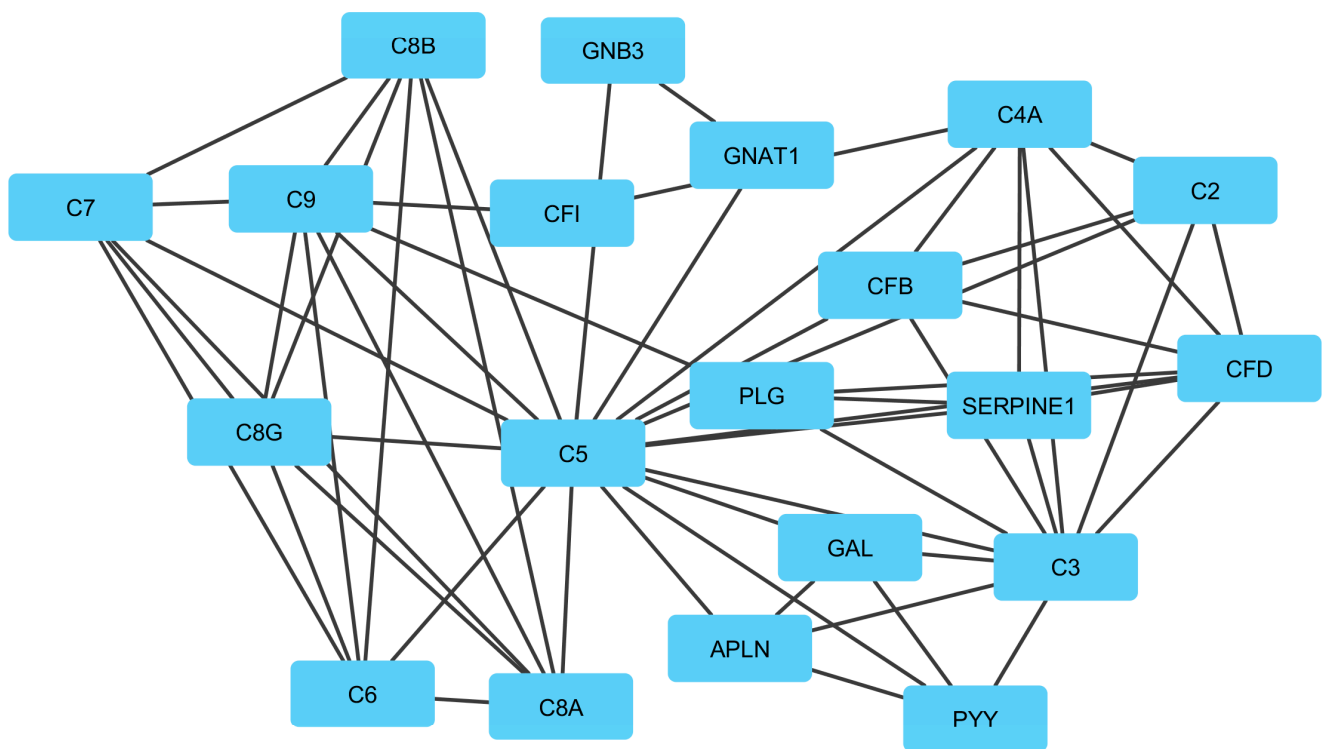


Figure 5. Module 2: 20 genes in an interactive network of genes. In this network, the quadrilateral nodes represent genes, and edges indicate the gene–gene interaction effects.

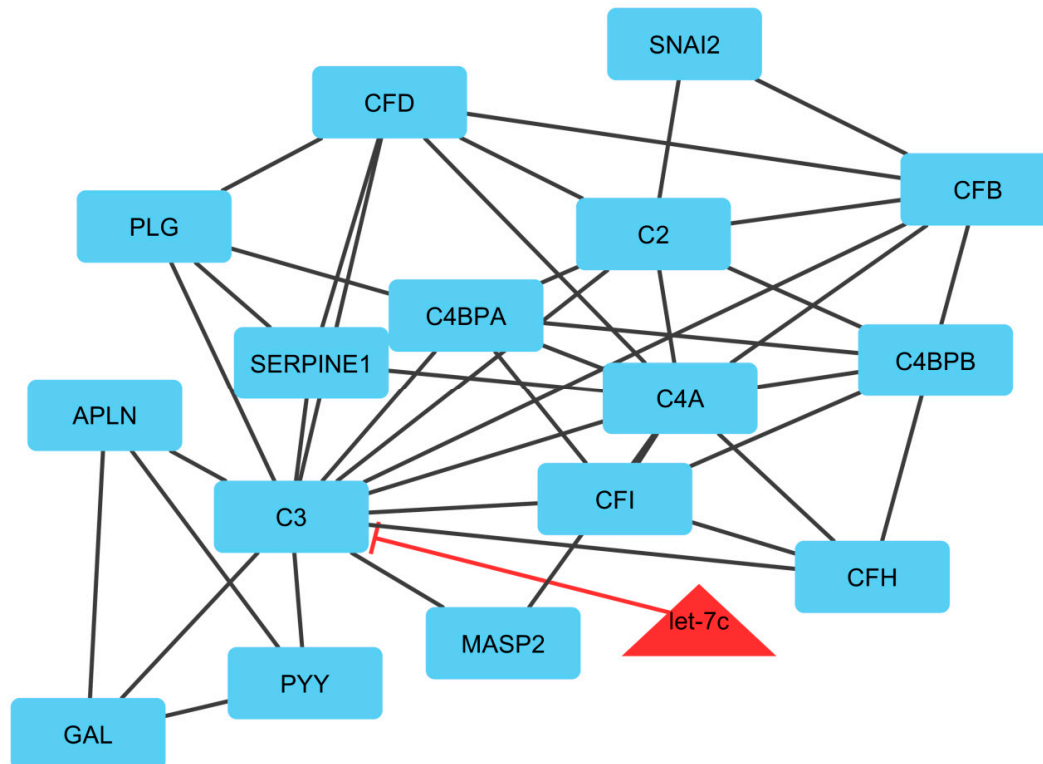


Figure 6. Module 3: 16 mRNAs/genes and 1 miRNA in an interacted network were identified. In this network, the quadrilateral nodes represent mRNAs/genes and triangle nodes represent miRNAs. Edges indicate the interactions; black edges represent mRNA–mRNA interactions and red edges represent miRNA–mRNA interactions.

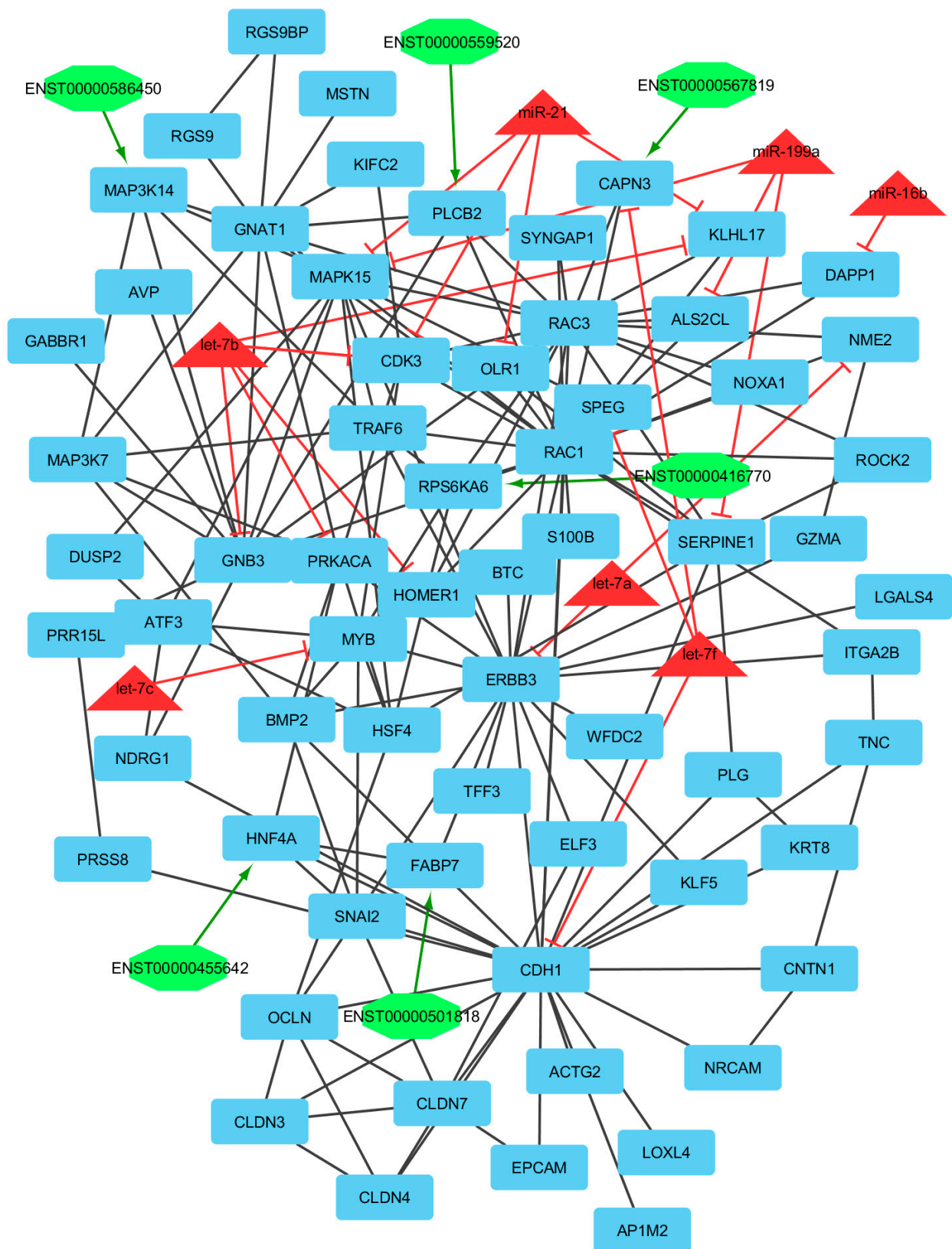


Figure 7. Module 4: 65 mRNAs/genes, 6 lncRNAs, and 7 miRNAs in an interacted network were identified. In this network, the quadrilateral nodes represent mRNAs/genes, octagonal nodes represent lncRNAs, and triangle nodes represent miRNAs. Edges indicate the interactions; black edges represent mRNA–mRNA interactions, green edges represent lncRNA–mRNA interactions, and red edges represent miRNA–mRNA interactions.

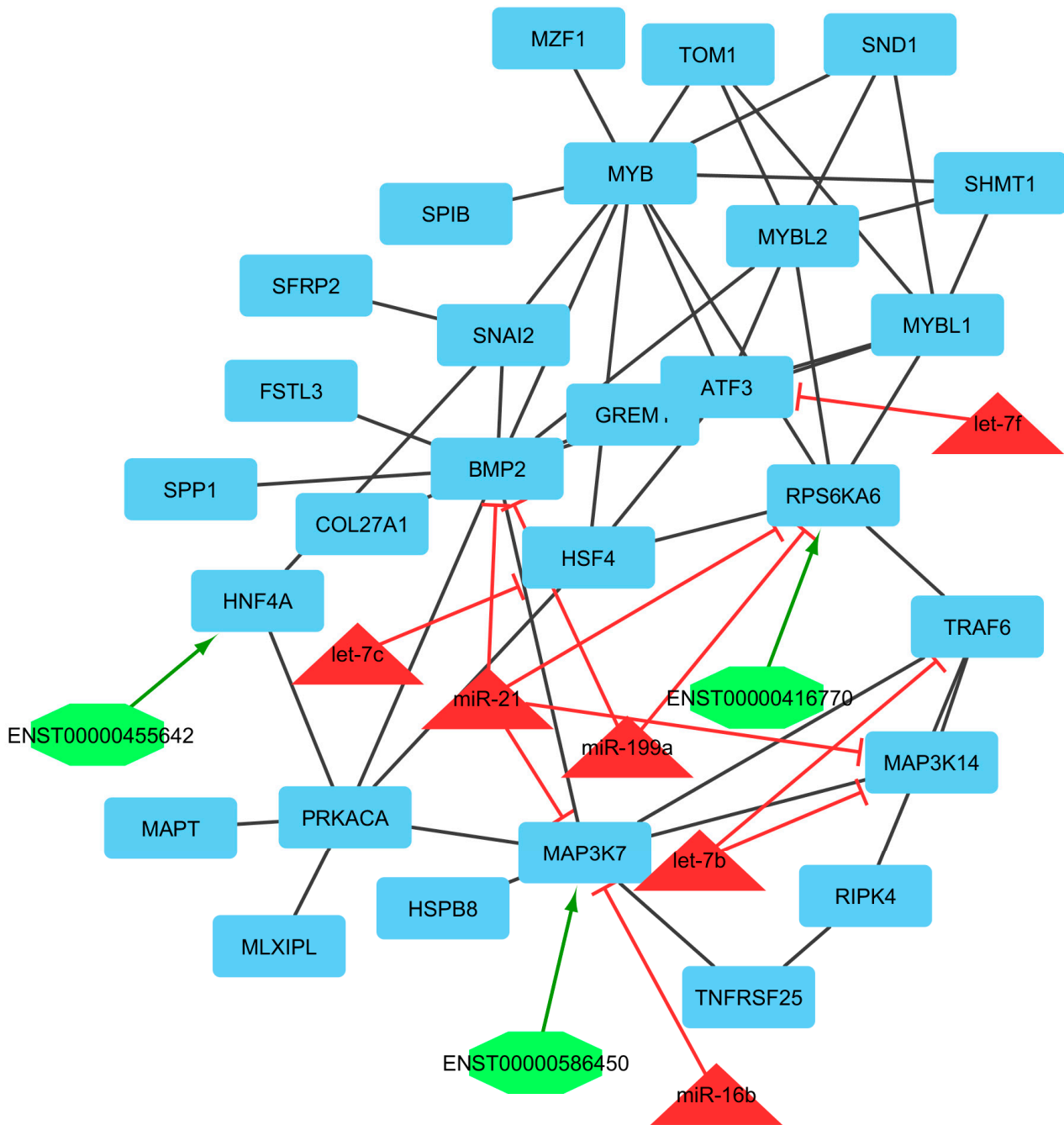


Figure 8. Module 5: 68 mRNAs/genes, 3 lncRNAs, and 6 miRNAs in an interacted network were identified. In this network, the quadrilateral nodes represent mRNAs/genes, octagonal nodes represent lncRNAs, and triangle nodes represent miRNAs. Edges indicate the interactions; black edges represent mRNA-mRNA interactions, green edges represent lncRNA-mRNA interactions, and red edges represent miRNA-mRNA interactions.

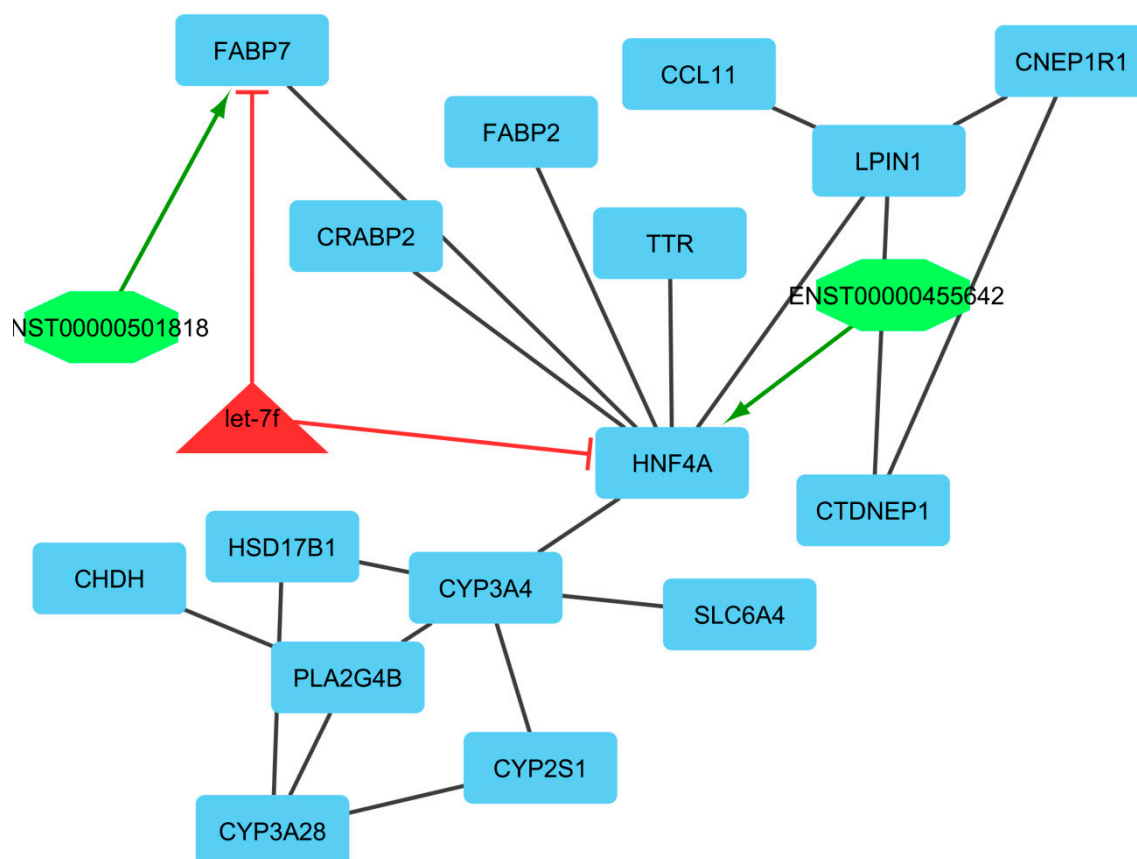


Figure 9. Module 6: 16 mRNAs/genes, 2 lncRNAs, and 1 miRNA in an interacted network were identified. In this network, the quadrilateral nodes represent mRNAs/genes, octagonal nodes represent lncRNAs, and triangle nodes represent miRNAs. Edges indicate the interactions; black edges represent mRNA–mRNA interactions, green edges represent lncRNA–mRNA interactions, and red edges represent miRNA–mRNA interactions.

4. Discussion

The whole-transcriptome profiling technique helps gain a more in-depth understanding of the functions of the corpus luteum, which may authorize the marker identification that is differentially expressed, for instance, between two breeds showing different litter size phenotypes. Although most of the investigations associated with pregnancy have been performed in sheep, only a few studies have used the whole-transcriptome approaches to the corpus luteum. Microarray-based transcriptomic research performed by Gray et al. (2006) identified several endometrial genes regulated by progesterone (from the corpus luteum). In a more comprehensive investigation performed by Brooks et al. [67], transcriptome analysis of corpus luteum during the peri-implantation period of pregnancy recognized different biological functions and regulatory pathways in sheep. Moore et al. [68] integrated GWAS with gene expression data to understand the roles of the corpus luteum transcriptomes in cattle fertility. Kfir et al. [69] recognized DEGs (differentially expressed genes) between day 4 and day 11 in the CL in dairy cows. Furthermore, an investigation of endometrial transcriptome differences between European mouflon and Finnsheep identified several transcripts associated with fertility [70]. Most studies just identify DEGs without recognizing associations among mRNAs/genes and considering other biological molecules including lncRNAs and miRNAs, whereas considering the interactions among all regulatory factors can provide an exhaustive understanding of the mechanisms involved in reproductive traits.

In 2011, Salmena et al. suggested the ceRNA (competitive endogenous RNA) hypothesis that lncRNAs and protein-coding RNAs can operate as competitive endogenous

RNAs to communicate by binding to miRNA sites [71,72]. According to the competitive endogenous RNAs hypothesis, many researchers have dedicated themselves to elucidating the competitive endogenous RNA roles of lncRNAs in some traits by constructing competitive endogenous RNA networks [73,74]. However, the entire regulatory network that links the processes of non-coding RNAs and coding has not been extensively explained. Collecting evidence proposes that lncRNA may operate as a competitive endogenous RNA for certain miRNAs to modulate the target mRNAs/genes of the miRNAs [75]. Several studies aiming to construct lncRNA-associated competitive endogenous RNA networks in production traits have been performed [76–78]. In this study, we first identified 264 differential expressed mRNAs, 34 differential expressed miRNAs, and 14 differentially expressed lncRNAs between CL samples of two different breeds. We finally constructed an lncRNA–miRNA–mRNA ceRNA network including 312 nodes and 748 lncRNA–miRNA–mRNA ceRNA interactions. Although we recognized potential mRNA–lncRNA and miRNA–mRNA interactions involved in prolificacy development by constructing a multi-partite network, a limitation in our analysis should be mentioned. The potential interactions were identified by prediction tools and RNA-seq; therefore, in the future, more experimental studies should be performed to validate the target predictions in sheep prolificacy development. The differentially expressed RNAs in the corpus luteum were involved in processes associated with proteolysis, actin cytoskeleton organization, immune system process, biological adhesion, cell differentiation, and lipid metabolic process. The computational method suggested in this study goes further by associating the various phases with ceRNA regulatory modules. The lncRNA–miRNA–mRNA ceRNA network defined in this study consists of mRNAs/genes, miRNA, and lncRNA and associated conditions in the indicated case. This potential approach provides a promising new opportunity to evaluate genetic traits such as the reproductive process by discovering ceRNA regulatory networks by linking different types of RNAs to different breeds or different groups. Understanding the molecular mechanism of fertility is needed to solve the complex synergies orchestrated during the process of reproduction. Although, several studies have described the presence of altered gene expression patterns in different reproductive processes [79–82].

Herein, we discovered several mRNAs/genes in the corpus luteum of high- and low-fertility sheep. Indeed, the role of these genes during fertility is not clearly understood yet, but some mRNAs/genes family members are believed to be involved in cell survival, proliferation, apoptosis, and other fundamental biological processes. The expression of these mRNAs/genes in both high-fertility and low-fertility in the corpus luteum could show their basal function cellular roles during the reproductive performance [83]. Our results have detected six candidate modules involved in sheep fertility, which are available in detail in Supplementary Table S8. These modules have detected 44, 7, and 7 mRNAs/genes, lncRNAs, and miRNAs (without repeated nodes), respectively, and modules 1, 2, 3, 4, 5, and 6 included 41, 20, 17, 78, 37, and 19 nodes, respectively, and, 129, 58, 42, 174, 60, and 22 interactions, respectively. Signaling pathway, biological process, and GO enrichment analysis of deregulated RNAs specified important biological processes, which are dysregulated by deregulated RNAs.

In module 1, let-7b, let-7a, let-7c, and miR-199a suppressed NOXA1, SYNGAP1, ROCK2, and PLCB2 genes, and almost all miRNAs were up-regulated, except let-7c, which was down-regulated and genes were down-regulated. Moreover, in this module, ENST00000416770, ENST00000567819, ENST00000559520, and ENST00000618857 interacted with RPS6KA6, CAPN3, PLCB2, and BACE1, respectively. The hub-hub genes included CAPN3, PLS1, CNN1, ACTA1, and KLHL17, in which PLS1, CNN1, and ACTA1 genes were up-regulated and CAPN3 and KLHL17 genes were down-regulated. All of these hub-hub genes are involved in the actin cytoskeleton organization process. Calpain 3 (CAPN3), a muscle-specific member of the calpain large subunit family that specifically binds to titin, has been suggested to be related to muscle growth in cattle and broiler chickens. Gene Ontology (GO) annotations related to this gene include calcium ion binding, peptidase activity, meat traits, and disease resistance [84]. PLCB2 gene interacted

with ENST00000559520 and both of them were down-regulated. Moreover, this gene was suppressed by miR-199a. PLCB2 encodes the protein that belong to phospholipases group and hydrolyze phospholipids into fatty acids and other lipophilic molecules. In animals, plastin 1 (PLS1) is a component of membrane signaling complexes controlling cell differentiation, motility, and adhesion, and has effects on calcium ion and actin filament binding [85]. Calponin 1 (CNN1) contributes to regulating contractility. This gene encoded cytoskeletal signaling and endothelin pathways. Moreover, it affects actin-binding and calmodulin-binding and is specifically expressed in smooth muscle cells [86,87]. Actin α 1 (ACTA1) gene encodes the thin filaments of the muscle contractile apparatus. This gene has a role in the structural constituent of the cytoskeleton, myosin binding, RhoGDI pathway, and cytoskeleton remodeling regulation of actin cytoskeleton by Rho GTPases [88]. Kelch like family member 17 (KLHL17) is an actin-binding protein that has a role in actin filament binding and POZ domain binding and is predominantly expressed in neurons of most regions of the brain [89]. A process that is fulfilling at the cellular level results in the arrangement, assembly of constituent parts, or disassembly of cytoskeletal structures comprising actin filaments and their related proteins [90].

In module 2, *C3*, *SERPINE1*, *CFB*, *C5*, and *CFI* genes were identified as the most important genes in that all of them were upregulated. The key biological process affected by these genes was the proteolysis process. The hydrolysis of proteins into amino acids or/and smaller polypeptides occurred by cleavage of their peptide bonds [91]. Serpin Family E Member 1 (*SERPINE1*) is a protein coding gene that has been determined to be transiently upregulated during the latter part of the estrous cycle and early luteolysis. Moreover, it may have a role in signaling receptor binding, protease binding, regulation of the extracellular matrix to facilitate the invasion of immune cells, and inhibiting the synthesis of progesterone [92]. Complement components C3 and C5 play a central role in the activation of the complement system. C5 (complement C5) is a gene encoding a protein of the innate immune system that had an important role in inflammation, host homeostasis, and host defense against pathogens. Some results present that many factors in the complement system (including C1, C3, C5, C6, C7, C8, and C9, as well as complement factor B and factor H) are regulated by heat stress in the blood [93]. Moreover, the complement system is a part of the body's immune system, which plays a key role in immune responses and defense against infection [94]. Complement factor B (*CFB*) of the alternative complement pathway has been identified in sheep as a major gene that has a key role in the regulation of the immune reaction, serine-type endopeptidase activity, and complement activation [95,96]. Complement Factor I (*CFI*) is a protein-coding gene that is related to the following pathways: immune response lectin induced complement pathway and the innate immune system [97].

In module 3, *let-7c* suppressed the *C3* gene and was down-regulated, and the mentioned gene was up-regulated. The hub-hub key genes involved in the immune system process were *C4BPB*, *SERPINE1*, *CFB*, *C4BPA*, and *MASP2*. *C3*, *C4BPB*, *SERPINE1*, *CFB*, and *C4BPA* genes were upregulated and *MASP2* gene was downregulated. *C4BP* gene binds strongly to apoptotic and necrotic cells and limits their complement activation. Complement component 4 binding protein β (*C4BPB*) and complement component 4 binding protein α (*C4BPA*) genes encode a member of a superfamily of proteins composed predominantly of tandemly arrayed short consensus repeats of approximately 60 amino acids. This gene has a major role in the innate immune system and immune response lectin induced complement pathways [98]. MBL associated serine protease 2 (*MASP2*) gene is associated with biological processes terms including acute inflammation and defense response. Activities related to this gene include calcium ion binding and peptidase activity [99]. Therefore, the biological process of these genes is involved in the functioning or development of the immune system and organismal system for calibrated responses to invasive or internal threats [100].

In module 4, miR-21, *let-7b*, *let-7a*, miR-16b, *let-7c*, *let-7f*, and miR-199a were identified. miR-21 suppressed *CDK3*, *KLHL17*, *MAPK15*, and *OLR1* genes and was downregulated.

let-7b suppressed *CDK3*, *GNB3*, *HOMER1*, *KLHL17*, *OLR1*, and *PRKACA* genes and was upregulated. let-7a suppressed *ERBB3* and *NME2* genes and was up-regulated. miR-16b suppressed the *DAPP1* gene and was up-regulated. let-7c suppressed the *MYB* gene and was down-regulated, and the *MYB* gene was up-regulated. let-7f suppressed *CAPN3*, *CDH1*, and *SPEG* genes and was down-regulated. miR-199a suppressed *ALS2CL*, *MAPK15*, and *SERPINE1* genes and was up-regulated. Moreover, in this module, ENST00000559520, ENST00000586450, ENST00000501818, ENST00000455642, and ENST00000567819 interacted with *PLCB2*, *MAP3K14*, *FABP7*, *HNF4A*, and *CAPN3*, respectively. The hub-hub genes included *ITGA2B*, *CDH1*, *SERPINE1*, *BMP2*, *TNC*, *NRCAM*, *CLDN3*, *CLDN4*, *MYB*, and *ERBB3*. Among these, *CDH1*, *SERPINE1*, *BMP2*, *TNC*, *NRCAM*, *CLDN3*, *CLDN4*, *MYB*, and *ERBB3* genes were upregulated and the *ITGA2B* gene was downregulated. Integrin subunit α 2b (*ITGA2B*) is a protein-coding gene that has a role in cytokine signaling in the immune system and RET signaling pathways and activities related to this gene including identical protein binding and fibrinogen binding. Moreover, for adhesion with this gene, integrins are known to participate in cell-surface mediated signaling [101]. Estradiol secretion by granulosa cells is generally increased in the presence of bone morphogenetic protein 2 (*BMP2*) in mammals [102,103]. Tenascin C (*TNC*) gene encodes an extracellular matrix protein with a spatially and temporally restricted tissue distribution. This gene has been reported to be involved in vertebrate neural, skeletal, and vascular morphogenesis during development as well as in the regulation of neuronal differentiation in the nervous system [104,105]. Neuronal cell adhesion molecule (*NRCAM*) is an Ig superfamily adhesion molecule that has a major role in L1CAM interactions and developmental biology pathways and ankyrin binding and protein binding are involved in heterotypic cell–cell adhesion [106]. Claudin 3 (*CLDN3*) is a protein-coding gene that has a key role in the blood–brain barrier and immune cell transmigration: *VCAM-1/CD106* signaling and cell junction organization. Moreover, *CLDN3*, *CLDN4*, and *MYB* genes are involved in modules associated with reproductive and fertility complex traits [105]. Erb-B2 receptor tyrosine kinase 3 (*ERBB3*) is a member of the epidermal growth factor receptor (*EGFR*) family of receptor tyrosine kinases that have a role during fetal ovary development in cows. Among its related pathways are NF-kappaB pathway and cytokine signaling in the immune system [107]. All of these genes are involved in the biological adhesion process. This involves the attachment of an organism/cell to a substrate/other organisms. Biological adhesion includes intracellular attachment between membrane regions.

In module 5, miR-21, let-7b, miR-16b, let-7c, let-7f, and miR-199a were identified. miR-21 suppressed *BMP2*, *MAP3K14*, *MAP3K7*, and *RPS6KA6* genes and was down-regulated. let-7b suppressed *MAP3K14* and *TRAF6* genes and was up-regulated. miR-16b suppressed the *MAP3K7* gene and was up-regulated. let-7c suppressed the *HSF4* gene and was down-regulated. let-7f suppressed the *ATF3* gene and was down-regulated. miR-199a suppressed *BMP2* and *RPS6KA6* genes and was up-regulated. Moreover, in this module, ENST00000455642, ENST00000416770, and ENST00000586450 interacted with *HNF4A*, *RPS6KA6*, and *MAP3K7*, respectively. *ATF3*, *HSF4*, *COL27A1*, *MYB*, *MAPT*, *SPIB*, *SFRP2*, *GREM1*, and *BMP2* genes were identified as hub-hub genes. Among these, *ATF3*, *MYB*, *SPIB*, *SFRP2*, and *GREM1* genes were up-regulated and *HSF4*, *COL27A1*, and *MAPT* genes were down-regulated. The key biological process affected by these genes was cell differentiation. The process includes unspecialized cells, for example, functional features that characterize the cells, embryonic/regenerative cells, and tissues/organs of the mature organism. Differentiation includes the processes involved in the obligation of a cell to a specific fate and its further development to the mature state [108]. Activating transcription factor 3 (*ATF3*) is an estrogen-responsive gene, a member of the mammalian activation transcription factor/cAMP-responsive element-binding (*CREB*) protein family of transcription factors. This gene has a role in PERK regulating gene expression and unfolded protein response (*UPR*) pathways [109]. Collagen type XXVII α 1 chain (*COL27A1*) gene is a member of the fibrillar collagen family and has a role in the calcification of cartilage and the transition of cartilage to bone [110]. Microtubule associated protein tau (*MAPT*) gene

promotes microtubule assembly and stability and might be involved in the establishment and maintenance of neuronal polarity [111]. Gremlin 1, DAN family BMP antagonist (GREM1) gene, encodes a member of the BMP (bone morphogenic protein) antagonist family and has a role in cytokine activity, BMP binding, and reproductive traits in Awassi sheep [112]. In this module, *MAP3K14* and *RPS6KA6* interacted with ENST00000586450 and ENST00000416770, respectively. All of them were down-regulated and were suppressed by miR-16b and miR-199a, which were up-regulated. *MAP3K14* encodes mitogen-activated protein kinase kinase kinase 14, which is a serine/threonine protein-kinase. This kinase binds to TRAF2 and stimulates NF-kappaB activity. It shares sequence similarity with several other MAPKK kinases. It participates in an NF-kappaB-inducing signalling cascade common to receptors of the tumour-necrosis/nerve-growth factor (TNF/NGF) family and to the interleukin-1 type-I receptor. Regardless, *RPS6KA6* encodes protein that constitutively activate serine/threonine-protein kinase, which exhibits growth-factor-independent kinase activity and may participate in p53/TP53-dependent cell growth arrest signaling and play an inhibitory role during embryogenesis.

In module 6, let-7f suppressed *FABP7* and *HNF4A* genes and was downregulated. Moreover, in this module, ENST00000455642 and ENST00000501818 interacted with *HNF4A* and *FABP7*, respectively. Hub-hub genes were *LPIN1*, *HSD17B1*, *PLA2G4B*, *CYP2S1*, *HNF4A*, *TTR*, and *CRABP2*. Among these, *HSD17B1*, *CYP2S1*, *HNF4A*, and *CRABP2* genes were upregulated and *LPIN1* and *PLA2G4B* genes were downregulated. Lipin 1 (*LPIN1*) is a member of the lipin family of proteins that has an important role in animal and poultry lipid metabolism and its regulation. This gene may have value as a genetic marker for improving some traits such as meat production and carcass [113]. The *HNF4A* gene interacted with ENST00000455642 and was highly upregulated, and suppressed by let-7f. This gene is a transcriptional regulator that controls the expression of some genes during the transition of endodermal cells to progenitor cells, facilitating the recruitment of RNA pol II to the promoters of target genes and activating the transcription of *CYP2C38*. It represses the CLOCK-ARNTL/BMAL1 transcriptional activity and is essential for circadian rhythm maintenance and period regulation in the some tissues cells. Hydroxysteroid 17- β dehydrogenase 1 (*HSD17B1*) is a gene that has a key role in the super pathway of steroid hormone biosynthesis and metabolism pathway. Moreover, the *HSD17B1* gene plays an essential role in the biological processes related to sheep ovulation [114]. Phospholipase A2 group IVB (*PLA2G4B*) gene encodes a member of the cytosolic phospholipase A2 protein family and has a role in calcium ion binding and phospholipase activity. This gene has been identified as one of the important genes in interaction networks in sheep fertility [115]. Cytochrome P450 family 2 subfamily S member 1 (*CYP2S1*) encodes a member of the cytochrome P450 superfamily of enzymes. *CYP2S1* gene is related to the reproductive processes as a regulatory factor in follicular development and ovarian development in the ovulation process in female mammals [116]. Therefore, most of these genes are involved in the lipid metabolic process. The chemical pathways and reactions involving lipid compounds soluble in an organic solvent include neutral fats, fatty acids and other fatty-acid esters, sphingoids and other long-chain bases, long-chain alcohols, waxes, phospholipids, glycolipids, and the other isoprenoids [117].

We offered a computational approach to an lncRNA-miRNA-mRNA ceRNA network using predicted and validated expression profiles of RNAs. Indeed, the use of the same breed might lead to more accurate results. However, these two sheep breeds are different, but in systemic studies, thresholds are usually considered that have the most genetic and phenotypic differences. The spatio-temporal differential expression in different tissues, especially CL, supports the potential role of RNAs in the transcriptional and post-transcriptional regulation of genes involved in prolificacy. The reports we presented here for the first time may be beneficial in discovering the basic molecular regulatory mechanisms of fertility in sheep. Although, further efforts are needed to discover the specific biological functional role of RNA modules during various stages of the reproductive traits. In addition, our findings showed that the integration of mRNAs, miRNAs, and lncRNAs

based on the ceRNA networks, along with different data such as lncRNA interactions, miRNA target prediction, PPI, and other regulatory networks, can be considered a robust approach to provide greater insights into biological processes at the molecular level.

5. Conclusions

This study applied a new approach to integrating different classes of RNA as an integrated network, and first reported transcriptome sequencing analysis of the corpus luteum in sheep. Integration of transcriptomic data for obtaining and identifying hub nodes with differences in expression levels led to the successful identification of 264 mRNAs/genes, 14 lncRNAs, and 34 miRNAs in the main process of prolificacy in the corpus luteum samples of Romanov compared with Baluchi breeds. Using lncRNA–miRNA–mRNA ceRNA network analysis and constructing the networks by merging the interactions and regulation networks, 6 key modules, 44 mRNAs/genes, 7 lncRNAs, and 7 miRNAs were identified as being involved in major biological processes including proteolysis, actin cytoskeleton organization, immune system process, biological adhesion, cell differentiation, and lipid metabolic process, and have an overexpression pattern. Overall, our results in this research demonstrate that integrated network analysis and the application of omics data of sheep corpus luteum generate novel insights into sheep fertility. Furthermore, a comparison of the transcriptomic level in these two breeds will be important for further genetic improvement of the trait and a better understanding of the molecular basis of reproduction in sheep as well as other mammals.

Supplementary Materials: The following supporting information can be downloaded at: <https://www.mdpi.com/article/10.3390/genes13081295/s1>, Figure S1: The result of reads correspondent to the AGR2 gene for validation of alignment related to transcripts, Table S1: Data for the phenotype of litter size of Ewes, Table S2: The primer pairs were designed using Geneious Prime software v2021.1, Table S3: The total RNAs in the different breeds that are known to be involved in prolificacy, Table S4: Detected the global gene expression that changed in CL, Table S5: Identified up-regulated and down-regulated miRNAs in Romanov with Baluchi (False discover rate, FDR < 0.05, fold change > 1.5 and P < 0.01), Table S6: Detected interactions for 312 nodes and 748 edges in the network, Table S7: The clusters were identified by ClusterONE and MCODE software and each cell color related to one cluster, Table S8: Detected 6 candidate modules involved in sheep fertility.

Author Contributions: Conceptualization, M.S., R.N. and A.B.; methodology, H.K. and M.S.; software, A.B. and S.A.A.; validation, H.K., A.H., R.N., M.S. and A.B.; formal analysis, A.B.; investigation, M.S.; resources, H.W.B.; writing—original draft preparation, A.B., A.H. and M.S.; writing—review and editing, A.H., R.N., F.G. and H.W.B.; visualization, A.H.; supervision, A.B. and H.W.B. All authors have read and agreed to the published version of the manuscript.

Funding: This research received no external funding.

Institutional Review Board Statement: The animal study was reviewed and approved by Animal Care Committee, University of Tehran.

Informed Consent Statement: Not applicable.

Data Availability Statement: All sequencing data have been submitted to the National Center for Biotechnology Information (NCBI) Gene Expression Omnibus (GEO). All data can be used without restrictions. Related accession number is GSE159902.

Acknowledgments: The authors thank all the teams who worked and provided technical assistance during this study. We also thank the anonymous reviewers whose critical comments helped in improving the manuscript.

Conflicts of Interest: The authors declare no conflict of interest.

References

1. Santolaria, P.; Palacin, I.; Yániz, J. Management factors affecting fertility in sheep. In *Artificial Insemination in Farm Animals*; IntechOpen: London, UK, 2011; pp. 167–190.
2. Dziuk, P.J.; Bellows, R.A. Management of reproduction of beef cattle, sheep and pigs. *Sci. J. Anim. Sci.* **1983**, *57*, 355–379.

3. Lucy, M.C. Reproductive loss in high-producing dairy cattle: Where will it end? *J. Dairy Sci.* **2001**, *84*, 1277–1293. [[CrossRef](#)]
4. Barbat, A.; Le Mézec, P.; Ducrocq, V.; Mattalia, S.; Fritz, S.; Boichard, D.; Ponsart, C.; Humblot, P. Female fertility in French dairy breeds: Current situation and strategies for improvement. *J. Reprod. Dev.* **2010**, *56*, 15–21. [[CrossRef](#)]
5. Davis, G.H. Major genes affecting ovulation rate in sheep. *Genet. Sel. Evol.* **2005**, *37*, S11–S23. [[CrossRef](#)] [[PubMed](#)]
6. Fahmy, M.H. *Prolific Sheep. Commonwealth Agricultural Bureau, Wallingford, OXON. Ox10 8DE, UK*; Elsevier: Amsterdam, The Netherlands, 1996.
7. Demars, J.; Fabre, S.; Sarry, J.; Rossetti, R.; Gilbert, H.; Persani, L.; Tosser-Klopp, G.; Mulsant, P.; Nowak, Z.; Drobik, W.; et al. Genome-wide association studies identify two novel BMP15 mutations responsible for an atypical hyperprolificacy phenotype in sheep. *PLoS Genet.* **2013**, *9*, e1003482. [[CrossRef](#)] [[PubMed](#)]
8. Bodin, L.; Di Pasquale, E.; Fabre, S.; Bontoux, M.; Monget, P.; Persani, L.; Mulsant, P. A novel mutation in the bone morphogenetic protein 15 gene causing defective protein secretion is associated with both increased ovulation rate and sterility in Lacaune sheep. *Endocrinology* **2007**, *148*, 393–400. [[CrossRef](#)]
9. Monteagudo, L.V.; Ponz, R.; Tejedor, M.T.; Laviña, A.; Sierra, I. A 17 bp deletion in the bone morphogenetic protein 15 (BMP15) gene is associated to increased prolificacy in the rasa Aragonesa sheep breed. *Anim. Reprod. Sci.* **2008**, *110*, 139–146. [[CrossRef](#)]
10. Chen, H.Y.; Shen, H.; Jia, B.; Zhang, Y.S.; Wang, X.H.; Zeng, X.C. Differential gene expression in ovaries of Qira black sheep and Hetian sheep using RNA-Seq technique. *PLoS ONE* **2015**, *10*, e0120170. [[CrossRef](#)]
11. Drouilhet, L.; Mansanet, C.; Sarry, J.; Tabet, K.; Bardou, P.; Woloszyn, F.; Lluch, J.; Harichaux, G.; Viguié, C.; Monniaux, D.; et al. The Highly 700 Prolific Phenotype of Lacaune Sheep Is Associated with an Ectopic Expression of the 701 B4GALNT2 Gene within the Ovary. *PLoS Genet.* **2013**, *9*, e1003809. [[CrossRef](#)]
12. Davis, G.H.; Farquhar, P.A.; O’Connell, A.R.; Everett-Hincks, J.M.; Wishart, P.J.; Galloway, S.M.; Dodds, K. A putative autosomal gene increasing ovulation rate in Romney sheep. *Anim. Reprod. Sci.* **2006**, *92*, 65–73. [[CrossRef](#)]
13. Chu, M.X.; Mu, Y.L.; Fang, L.; Ye, S.C.; Sun, S.H. Prolactin receptor as a candidate gene for prolificacy of small tail Han sheep. *Anim. Biotechnol.* **2007**, *18*, 65–73. [[CrossRef](#)] [[PubMed](#)]
14. Xu, S.S.; Gao, L.; Xie, X.L.; Ren, Y.L.; Shen, Z.Q.; Wang, F.; Shen, M.; Eyþórsdóttir, E.; Hallsson, J.H.; Kiseleva, T.; et al. Genome-Wide Association Analyses Highlight the Potential for Different Genetic Mechanisms for Litter Size Among Sheep Breeds. *Front. Genet.* **2018**, *9*, 118. [[CrossRef](#)] [[PubMed](#)]
15. Hanrahan, J.P.; Quirke, J.F. Contribution of variation in ovulation rate and embryo survival to within breed variation in litter size. *Genet. Reprod. Sheep* **1984**, 193–201. [[CrossRef](#)]
16. Pokharel, K.; Peippo, J.; Honkatukia, M.; Seppälä, A.; Rautiainen, J.; Ghanem, N.; Hamama, T.M.; Crowe, M.A.; Andersson, M.; Li, M.H.; et al. Integrated ovarian mRNA and miRNA transcriptome profiling characterizes the genetic basis of prolificacy traits in sheep (*Ovis aries*). *BMC Genom.* **2018**, *19*, 104. [[CrossRef](#)]
17. Spencer, T.E.; Johnson, G.A.; Bazer, F.W.; Burghardt, R.C.; Palmarini, M. Pregnancy recognition and conceptus implantation in domestic ruminants: Roles of progesterone, interferons and endogenous retroviruses. *Reprod. Fertil. Dev.* **2007**, *19*, 65–78. [[CrossRef](#)] [[PubMed](#)]
18. Safari, E.; Fogarty, N.M.; Gilmour, A.R. A review of genetic parameter estimates for wool, growth, meat and reproduction traits in sheep. *Livest. Prod. Sci.* **2005**, *92*, 271–289. [[CrossRef](#)]
19. Bahrami, A.; Miraie-Ashtiani, S.R.; Sadeghi, M.; Najafi, A. miRNA-mRNA network involved in folliculogenesis interactome: Systems biology approach. *Reproduction* **2017**, *154*, 51–65. [[CrossRef](#)]
20. Ghafouri, F.; Bahrami, A.; Sadeghi, M.; Miraie-Ashtiani, S.R.; Bakherad, M.; Barkema, H.W.; Larose, S. Omics multi-layers networks provide novel mechanistic and functional insights into fat storage and lipid metabolism in poultry. *Front. Genet.* **2021**, *12*, 646297. [[CrossRef](#)]
21. Miao, X.; Luo, Q.; Zhao, H.; Qin, X. An integrated analysis of miRNAs and methylated genes encoding mRNAs and lncRNAs in sheep breeds with different fecundity. *Front. Physiol.* **2017**, *8*, 1049. [[CrossRef](#)]
22. Long, J.A. The ‘omics’ revolution: Use of genomic, transcriptomic, proteomic and metabolomic tools to predict male reproductive traits that impact fertility in livestock and poultry. *Anim. Reprod. Sci.* **2020**, *220*, 106354. [[CrossRef](#)]
23. Walsh, S.W.; Williams, E.J.; Evans, A.C.O. A review of the causes of poor fertility in high milk producing dairy cows. *Anim. Reprod. Sci.* **2011**, *123*, 127–138. [[CrossRef](#)] [[PubMed](#)]
24. Forde, N.; Mehta, J.P.; McGettigan, P.A.; Mamo, S.; Bazer, F.W.; Spencer, T.E.; Lonergan, P. Alterations in expression of endometrial genes coding for proteins secreted into the uterine lumen during conceptus elongation in cattle. *BMC Genom.* **2013**, *14*, 1–13. [[CrossRef](#)] [[PubMed](#)]
25. Forde, N.; McGettigan, P.A.; Mehta, J.P.; O’Hara, L.; Mamo, S.; Bazer, F.W.; Spencer, T.E.; Lonergan, P. Proteomic analysis of uterine fluid during the pre-implantation period of pregnancy in cattle. *Reproduction* **2014**, *147*, 575–587. [[CrossRef](#)]
26. Forde, N.; Simintiras, C.A.; Sturme, R.; Mamo, S.; Kelly, A.K.; Spencer, T.E.; Bazer, F.W.; Lonergan, P. Amino acids in the uterine luminal fluid reflects the temporal changes in transporter expression in the endometrium and conceptus during early pregnancy in cattle. *PLoS ONE* **2014**, *9*, e100010. [[CrossRef](#)]
27. Robinson, R.S.; Woad, K.J.; Hunter, M.G.; Sinclair, K.D.; Laird, M.; Joseph, C.; Hammond, A.J.; Mann, G.E. Corpus luteum development and angiogenesis. In *Reproduction in Domestic Ruminants VIII, Proceedings of the Ninth International Symposium on Reproduction in Domestic Ruminants, Obihiro, Hokkaido, Japan, August 2014*; Context Products Limited: London, UK, 2014; Volume 1, pp. 327–343.

28. Robinson, M.D.; McCarthy, D.J.; Smyth, G.K. edgeR: A Bioconductor package for differential expression analysis of digital gene expression data. *Bioinformatics* **2010**, *26*, 139–140. [CrossRef]
29. Miao, X.; Luo, Q.; Zhao, H.; Qin, X. Co-expression analysis and identification of fecundity-related long non-coding RNAs in sheep ovaries. *Sci. Rep.* **2016**, *6*, 39398. [CrossRef] [PubMed]
30. Hasankhani, A.; Bahrami, A.; Sheybani, N.; Fatehi, F.; Abadeh, R.; Ghaem Maghami Farahani, H.; Bahreini Behzadi, M.R.; Javanmard, G.; Isapour, S.; Khadem, H.; et al. Integrated Network Analysis to Identify Key Modules and Potential Hub Genes Involved in Bovine Respiratory Disease: A Systems Biology Approach. *Front. Genet.* **2021**, *12*, 753839. [CrossRef]
31. La, Y.; Tang, J.; He, X.; Di, R.; Wang, X.; Liu, Q.; Zhang, L.; Zhang, X.; Zhang, J.; Hu, W.; et al. Identification and characterization of mRNAs and lncRNAs in the uterus of polytocous and monotocous Small Tail Han sheep (*Ovis aries*). *PeerJ* **2019**, *7*, e6938. [CrossRef]
32. Chen, L.; Li, W.; Zhang, L.; Wang, H.; He, W.; Tai, J.; Li, X.; Li, X. Disease gene interaction pathways: A potential framework for how disease genes associate by disease-risk modules. *PLoS ONE* **2011**, *6*, e24495. [CrossRef]
33. Bugrim, A.; Nikolskaya, T.; Nikolsky, Y. Early prediction of drug metabolism and toxicity: Systems biology approach and modeling. *Drug Discov. Today* **2004**, *9*, 127–135. [CrossRef]
34. Kitano, H.; Funahashi, A.; Matsuoka, Y.; Oda, K. Using process diagrams for the graphical representation of biological networks. *Nat. Biotechnol.* **2005**, *23*, 961–966. [CrossRef]
35. Kann, M.G. Protein interactions and disease: Computational approaches to uncover the etiology of diseases. *Brief. Bioinform.* **2007**, *8*, 333–346. [CrossRef] [PubMed]
36. Morris, K.V.; Mattick, J.S. The rise of regulatory RNA. *Nat. Rev. Genet.* **2014**, *15*, 423–437. [CrossRef] [PubMed]
37. Wei, S.; Min, D.; Jiang, Z.; Hausman, G.J.; Zhang, L.; Dodson, M.V. Long noncoding RNAs in regulating adipogenesis: New RNAs shed lights on obesity. *Cell Mol. Life Sci.* **2016**, *73*, 2079–2087. [CrossRef] [PubMed]
38. Wang, W.; Zhang, E.; Lin, C. MicroRNAs in tumor angiogenesis. *Life Sci.* **2015**, *136*, 28–35. [CrossRef] [PubMed]
39. Wheelock, C.E.; Wheelock, Å.M.; Kawashima, S.; Diez, D.; Kanehisa, M.; van Erk, M.; Kleemann, R.; Haeggström, J.Z.; Goto, S. Systems biology approaches and pathway tools for investigating cardiovascular disease. *Mol. Biosyst.* **2009**, *5*, 588–602. [CrossRef]
40. Hallock, P.; Thomas, M.A. Integrating the Alzheimer’s disease proteome and transcriptome: A comprehensive network model of a complex disease. *Omics J. Integr. Biol.* **2012**, *16*, 37–49. [CrossRef]
41. Yazdi, M.H.; Eftekhari-Shahroudi, F.; Hejazi, M.; Liljedahl, L.E. Environmental effects on growth traits and fleece weights in Baluchi sheep. *J. Anim. Breed. Genet.* **1998**, *115*, 455–465. [CrossRef]
42. Herlihy, M.M.; Crowe, M.A.; Diskin, M.G.; Butler, S.T. Effects of synchronization treatments on ovarian follicular dynamics, corpus luteum growth, and circulating steroid hormone concentrations in lactating dairy cows. *J. Dairy Sci.* **2012**, *95*, 743–754. [CrossRef]
43. Kot, K.; Anderson, L.E.; Tsai, S.J.; Wiltbank, M.C.; Ginther, O.J. Transvaginal, ultrasound-guided biopsy of the corpus luteum in cattle. *Theriogenology* **1999**, *52*, 987–993. [CrossRef]
44. Chomczynski, P.; Sacchi, N. Single-step method of RNA isolation by acid guanidinium thiocyanate-phenol-chloroform extraction. *Anal. Biochem.* **1987**, *162*, 156–159. [CrossRef]
45. Blankenberg, D.; Gordon, A.; Von Kuster, G.; Coraor, N.; Taylor, J.; Nekrutenko, A.; Galaxy Team. Manipulation of FASTQ data with Galaxy. *Bioinformatics* **2010**, *26*, 1783–1785. [CrossRef]
46. Andrews, S. FastQC: A Quality Control Tool for High Throughput Sequence Data. Available online: <https://www.sciencedirect.com/science/article/pii/S0003269718300630> (accessed on 20 December 2021).
47. Bolger, A.M.; Lohse, M.; Usadel, B. Trimmomatic: A flexible trimmer for Illumina sequence data. *Bioinformatics* **2014**, *30*, 2114–2120. [CrossRef]
48. Kim, D.; Langmead, B.; Salzberg, S.L. HISAT: A fast spliced aligner with low memory requirements. *Nat. Methods* **2015**, *12*, 357–360. [CrossRef]
49. Trapnell, C.; Williams, B.A.; Pertea, G.; Mortazavi, A.; Kwan, G.; Van Baren, M.J.; Salzberg, S.L.; Wold, B.J.; Pachter, L. Transcript assembly and quantification by RNA-Seq reveals unannotated transcripts and isoform switching during cell differentiation. *Nat. Biotechnol.* **2010**, *28*, 511–515. [CrossRef]
50. Liao, Y.; Smyth, G.K.; Shi, W. featureCounts: An efficient general purpose program for assigning sequence reads to genomic features. *Bioinformatics* **2014**, *30*, 923–930. [CrossRef]
51. Love, M.I.; Huber, W.; Anders, S. Moderated estimation of fold change and dispersion for RNA-seq data with DESeq2. *Genome Biol.* **2014**, *15*, 550. [CrossRef]
52. Robinson, J.T.; Thorvaldsdóttir, H.; Winckler, W.; Guttman, M.; Lander, E.S.; Getz, G.; Mesirov, J.P. Integrative genomics viewer. *Nat. Biotechnol.* **2011**, *29*, 24–26. [CrossRef]
53. Raudvere, U.; Kolberg, L.; Kuzmin, I.; Arak, T.; Adler, P.; Peterson, H.; Vilo, J. g:Profiler: A web server for functional enrichment analysis and conversions of gene lists (2019 update). *Nucleic Acids Res.* **2019**, *47*, 191–198. [CrossRef]
54. Szklarczyk, D.; Gable, A.L.; Lyon, D.; Junge, A.; Wyder, S.; Huerta-Cepas, J.; Simonovic, M.; Doncheva, N.T.; Morris, J.H.; Bork, P.; et al. STRING v11: Protein–protein association networks with increased coverage, supporting functional discovery in genome-wide experimental datasets. *Nucleic Acids Res.* **2019**, *47*, 607–613. [CrossRef]
55. Huang, D.W.; Sherman, B.T.; Lempicki, R.A. Systematic and integrative analysis of large gene lists using DAVID bioinformatics resources. *Nat. Protoc.* **2009**, *4*, 44–57. [CrossRef]

56. Zhao, Y.; Li, H.; Fang, S.; Kang, Y.; Wu, W.; Hao, Y.; Li, Z.; Bu, D.; Sun, N.; Zhang, M.Q.; et al. Noncode 2016: An informative and valuable data source of long non-coding rnas. *Nucleic Acids Res.* **2015**, *44*, D203–D208. [[CrossRef](#)]
57. Volders, P.J.; Anckaert, J.; Verheggen, K.; Nuytens, J.; Martens, L.; Mestdagh, P.; Vandesompele, J. Lncipedia 5: Towards a reference set of human long non-coding rnas. *Nucleic Acids Res.* **2018**, *47*, D135–D139. [[CrossRef](#)]
58. Bader, G.D.; Cary, M.P.; Sander, C. Pathguide: A pathway resource list. *Nucleic Acids Res.* **2006**, *34* (Suppl. S1), 504–506. [[CrossRef](#)]
59. Xenarios, I.; Salwinski, L.; Duan, X.J.; Higney, P.; Kim, S.M.; Eisenberg, D. DIP, the Database of Interacting Proteins: A research tool for studying cellular networks of protein interactions. *Nucleic Acids Res.* **2002**, *30*, 303–305. [[CrossRef](#)]
60. Bader, G.D.; Donaldson, I.; Wolting, C.; Ouellette, B.F.; Pawson, T.; Hogue, C.W. BIND—the biomolecular interaction network database. *Nucleic Acids Res.* **2001**, *29*, 242–245. [[CrossRef](#)]
61. Pagel, P.; Kovac, S.; Oesterheld, M.; Brauner, B.; Dunger-Kaltenbach, I.; Frishman, G.; Montrone, C.; Mark, P.; Stümpflen, V.; Mewes, H.W.; et al. The MIPS mammalian protein–protein interaction database. *Bioinformatics* **2005**, *21*, 832–834. [[CrossRef](#)]
62. Chatr-Aryamontri, A.; Breitkreutz, B.J.; Heinicke, S.; Boucher, L.; Winter, A.; Stark, C.; Nixon, J.; Ramage, L.; Kolas, N.; O'Donnell, L.; et al. The BioGRID interaction database: 2013 update. *Nucleic Acids Res.* **2012**, *41*, 816–823. [[CrossRef](#)]
63. Mostafavi, S.; Ray, D.; Warde-Farley, D.; Grouios, C.; Morris, Q. GeneMANIA: A real-time multiple association network integration algorithm for predicting gene function. *Genome Biol.* **2008**, *9*, S4. [[CrossRef](#)]
64. Mi, H.; Muruganujan, A.; Thomas, P.D. PANTHER in 2013: Modeling the evolution of gene function, and other gene attributes, in the context of phylogenetic trees. *Nucleic Acids Res.* **2012**, *41*, 377–386. [[CrossRef](#)]
65. Shannon, P.; Markiel, A.; Ozier, O.; Baliga, N.S.; Wang, J.T.; Ramage, D.; Amin, N.; Schwikowski, B.; Ideker, T. Cytoscape: A software environment for integrated models of biomolecular interaction networks. *Genome Res.* **2003**, *13*, 2498–2504. [[CrossRef](#)] [[PubMed](#)]
66. Nepusz, T.; Yu, H.; Paccanaro, A. Detecting overlapping protein complexes in protein-protein interaction networks. *Nat. Methods* **2012**, *9*, 471–472. [[CrossRef](#)]
67. Bader, G.D.; Hogue, C.W. An automated method for finding molecular complexes in large protein interaction networks. *BMC Bioinform.* **2003**, *4*, 2. [[CrossRef](#)] [[PubMed](#)]
68. Gray, C.A.; Abbey, C.A.; Beremand, P.D.; Choi, Y.; Farmer, J.L.; Adelson, D.L.; Thomas, T.L.; Bazer, F.W.; Spencer, T.E. Identification of Endometrial Genes Regulated by Early Pregnancy, Progesterone, and Interferon Tau in the Ovine Uterus. *Biol. Reprod.* **2006**, *74*, 383–394. [[CrossRef](#)]
69. Brooks, K.; Burns, G.W.; Moraes, J.G.N.; Spencer, T.E. Analysis of the Uterine Epithelial and Conceptus Transcriptome and Luminal Fluid Proteome During the Peri Implantation Period of Pregnancy in Sheep. *Biol. Reprod.* **2016**, *95*, 88. [[CrossRef](#)]
70. Moore, S.G.; Pryce, J.E.; Hayes, B.J.; Chamberlain, A.J.; Kemper, K.E.; Berry, D.P.; McCabe, M.; Cormican, P.; Lonergan, P.; Fair, T.; et al. Differentially Expressed Genes in Endometrium and Corpus Luteum of Holstein Cows Selected for High and Low Fertility Are Enriched for Sequence Variants Associated with Fertility1. *Biol. Reprod.* **2016**, *94*, 1–11. [[CrossRef](#)] [[PubMed](#)]
71. Kfir, S.; Basavaraja, R.; Wigoda, N.; Ben-Dor, S.; Orr, I.; Meidan, R. Genomic profiling 773 of bovine corpus luteum maturation. *PLoS ONE* **2018**, *13*, e0194456. [[CrossRef](#)] [[PubMed](#)]
72. Yang, J.; Li, X.; Cao, Y.H.; Pokharel, K.; Hu, X.J.; Chen, Z.H.; Xu, S.-S.; Peippo, J.; Honkatukia, M.; Kantanen, J.; et al. Comparative mRNA and miRNA expression in European mouflon (*Ovis musimon*) and sheep (*Ovis aries*) provides novel insights into the genetic mechanisms for female reproductive success. *Heredity* **2019**, *122*, 172–186. [[CrossRef](#)]
73. Salmena, L.; Poliseno, L.; Tay, Y.; Kats, L.; Pandolfi, P.P. A ceRNA hypothesis: The Rosetta Stone of a hidden RNA language? *Cell* **2011**, *146*, 353–358. [[CrossRef](#)]
74. Han, R.; Han, L.; Wang, S.; Li, H. Whole Transcriptome Analysis of Mesenchyme Tissue in Sika Deer Antler Revealed the CeRNAs Regulatory Network Associated With Antler Development. *Front. Genet.* **2020**, *10*, 1403. [[CrossRef](#)]
75. Li, H.; Huang, K.; Wang, P.; Feng, T.; Shi, D.; Cui, K.; Luo, C.; Shafique, L.; Qian, Q.; Ruan, J.; et al. Comparison of Long-Coding RNA Expression Profiles of Cattle and Buffalo Differing in Muscle Characteristics. *Front. Genet.* **2020**, *11*, 98. [[CrossRef](#)] [[PubMed](#)]
76. Wang, J.; Ren, Q.; Hua, L.; Chen, J.; Zhang, J.; Bai, H.; Li, H.; Xu, B.; Shi, Z.; Cao, H.; et al. Comprehensive Analysis of Differentially Expressed mRNA, lncRNA and circRNA and Their ceRNA Networks in the Longissimus Dorsi Muscle of Two Different Pig Breeds. *Int. J. Mol. Sci.* **2019**, *20*, 1107. [[CrossRef](#)] [[PubMed](#)]
77. Fan, H.; Ge, Y.; Ma, X.; Li, Z.; Shi, L.; Lin, L.; Xiao, J.; Chen, W.; Ni, P.; Yang, L.; et al. Long non-coding RNA CCDC144NL-AS1 sponges miR-143-3p and regulates MAP3K7 by acting as a competing endogenous RNA in gastric cancer. *Cell Death Dis.* **2020**, *11*, 521. [[CrossRef](#)] [[PubMed](#)]
78. Shi, T.; Hu, W.; Hou, H.; Zhao, Z.; Shang, M.; Zhang, L. Identification and Comparative Analysis of Long Non-Coding RNA in the Skeletal Muscle of Two Dezhou Donkey Strains. *Genes* **2020**, *11*, 508. [[CrossRef](#)]
79. Sun, J.; Xie, M.; Huang, Z.; Li, H.; Chen, T.; Sun, R.; Wang, J.; Xi, Q.; Wu, T.; Zhang, Y. Integrated analysis of non-coding RNA and mRNA expression profiles of 2 pig breeds differing in muscle traits. *J. Anim. Sci.* **2017**, *95*, 1092–1103. [[CrossRef](#)]
80. Yue, B.; Li, H.; Liu, M.; Wu, J.; Li, M.; Lei, C.; Huang, B.; Chen, H. Characterization of lncRNA–miRNA–mRNA Network to Reveal Potential Functional ceRNAs in Bovine Skeletal Muscle. *Front. Genet.* **2019**, *10*, 91. [[CrossRef](#)]
81. Bao, B.; Garverick, H.A. Expression of steroidogenic enzyme and gonadotropin receptor genes in bovine follicles during ovarian follicular waves: A review. *J. Anim. Sci.* **1998**, *76*, 1903–1921. [[CrossRef](#)]

82. Vitt, U.A.; Hayashi, M.; Klein, C.; Hsueh, A.J.W. Growth differentiation factor-9 stimulates proliferation but suppresses the follicle-stimulating hormone-induced differentiation of cultured granulosa cells from small antral and preovulatory rat follicles. *Biol. Reprod.* **2000**, *62*, 370–377. [[CrossRef](#)]
83. Hayashi, K.G.; Ushizawa, K.; Hosoe, M.; Takahashi, T. Differential genome-wide gene expression profiling of bovine largest and second-largest follicles: Identification of genes associated with growth of dominant follicles. *Reprod. Biol. Endocrinol.* **2010**, *8*, 11. [[CrossRef](#)]
84. Turcatel, G.; Rubin, N.; El-Hashash, A.; Warburton, D. MIR-99a and MIR-99b modulate TGF- β induced epithelial to mesenchymal plasticity in normal murine mammary gland cells. *PLoS ONE* **2012**, *7*, e31032. [[CrossRef](#)]
85. Zhang, Y.; Xue, X.; Liu, Y.; Abied, A.; Ding, Y.; Zhao, S.; Wang, W.; Ma, L.; Guo, J.; Guan, W.; et al. Genome-wide comparative analyses reveal selection signatures underlying adaptation and production in Tibetan and Poll Dorset sheep. *Sci. Rep.* **2021**, *11*, 2466. [[CrossRef](#)] [[PubMed](#)]
86. Clergeot, P.H.; Gourgues, M.; Cots, J.; Laurans, F.; Latorse, M.P.; Pépin, R.; Tharreau, D.; Notteghem, J.L.; Lebrun, M.H. PLS1, a gene encoding a tetraspanin-like protein, is required for penetration of rice leaf by the fungal pathogen *Magnaporthe grisea*. *Proc. Natl. Acad. Sci. USA* **2001**, *98*, 6963–6968. [[CrossRef](#)] [[PubMed](#)]
87. Feng, H.Z.; Wang, H.; Takahashi, K.; Jin, J.P. Double deletion of calponin 1 and calponin 2 in mice decreases systemic blood pressure with blunted length-tension response of aortic smooth muscle. *J. Mol. Cell. Cardiol.* **2019**, *129*, 49–57. [[CrossRef](#)]
88. Plazyo, O.; Hao, W.; Jin, J.P. The absence of calponin 2 in rabbits suggests caution in choosing animal models. *Front. Bioeng. Biotechnol.* **2020**, *8*, 42. [[CrossRef](#)] [[PubMed](#)]
89. Noce, A.; Cardoso, T.F.; Manunza, A.; Martínez, A.; Cánovas, A.; Pons, A.; Bermejo, L.A.; Landi, V.; Sánchez, A.; Jordana, J.; et al. Expression patterns and genetic variation of the ovine skeletal muscle transcriptome of sheep from five Spanish meat breeds. *Sci. Rep.* **2018**, *8*, 10486. [[CrossRef](#)] [[PubMed](#)]
90. Hu, H.T.; Huang, T.N.; Hsueh, Y.P. KLHL17/Actinfilin, a brain-specific gene associated with infantile spasms and autism, regulates dendritic spine enlargement. *J. Biomed. Sci.* **2020**, *27*, 103. [[CrossRef](#)] [[PubMed](#)]
91. Villanueva, M.A.; Arzápalo-Castañeda, G.; Castillo-Medina, R.E. The actin cytoskeleton organization and disorganization properties of the photosynthetic dinoflagellate *Symbiodinium kawagutii* in culture. *Can. J. Microbiol.* **2014**, *60*, 767–775. [[CrossRef](#)] [[PubMed](#)]
92. Wernimont, A.; Edwards, A. In situ proteolysis to generate crystals for structure determination: An update. *PLoS ONE* **2009**, *4*, e5094. [[CrossRef](#)]
93. Romero, J.J.; Antoniazzi, A.Q.; Smirnova, N.P.; Webb, B.T.; Yu, F.; Davis, J.S.; Hansen, T.R. Pregnancy-associated genes contribute to antiluteolytic mechanisms in ovine corpus luteum. *Physiol. Genom.* **2013**, *45*, 1095–1108. [[CrossRef](#)]
94. Min, L.; Cheng, J.; Zhao, S.; Tian, H.; Zhang, Y.; Li, S.; Yang, H.; Zheng, N.; Wang, J. Plasma-based proteomics reveals immune response, complement and coagulation cascades pathway shifts in heat-stressed lactating dairy cows. *J. Proteom.* **2016**, *146*, 99–108. [[CrossRef](#)]
95. Carroll, M.C. Complement and humoral immunity. *Vaccine* **2008**, *26*, 28–33. [[CrossRef](#)] [[PubMed](#)]
96. Qin, J.; Munyard, K.; Lee, C.Y.; Wetherall, J.D.; Groth, D.M. Characterization of the sheep Complement Factor B gene (CFB). *Vet. Immunol. Immunopathol.* **2011**, *140*, 170–174. [[CrossRef](#)] [[PubMed](#)]
97. Serrano, M.; Ramón, M.; Calvo, J.H.; Jiménez, M.Á.; Freire, F.; Vázquez, J.M.; Arranz, J.J. Genome-wide association studies for sperm traits in Assaf sheep breed. *Animal* **2021**, *15*, 100065. [[CrossRef](#)]
98. Timár, K.K.; Junnikkala, S.; Dallos, A.; Jarva, H.; Bhuiyan, Z.A.; Meri, S.; Bos, J.D.; Asghar, S.S. Human keratinocytes produce the complement inhibitor factor I: Synthesis is regulated by interferon- γ . *Mol. Immunol.* **2007**, *44*, 2943–2949. [[CrossRef](#)]
99. Mohlin, F.C.; Mercier, E.; Fremeaux-Bacchi, V.; Liszewski, M.K.; Atkinson, J.P.; Gris, J.C.; Blom, A.M. Analysis of genes coding for CD 46, CD 55, and C 4b-binding protein in patients with idiopathic, recurrent, spontaneous pregnancy loss. *Eur. J. Immunol.* **2013**, *43*, 1617–1629. [[CrossRef](#)]
100. Ha, M.; Sabherwal, M.; Duncan, E.; Stevens, S.; Stockwell, P.; McConnell, M.; Bekhit, A.E.D.; Carne, A. In-depth characterization of sheep (*Ovis aries*) milk whey proteome and comparison with cow (*Bos taurus*). *PLoS ONE* **2015**, *10*, e0139774. [[CrossRef](#)]
101. Beck, G.; Habicht, G.S. Immunity and the invertebrates. *Sci. Am.* **1996**, *275*, 60–66. [[CrossRef](#)] [[PubMed](#)]
102. Khoriaty, R.; Ozel, A.B.; Ramdas, S.; Ross, C.; Desch, K.; Shavit, J.A.; Everett, L.; Siemieniak, D.; Li, J.Z.; Ginsburg, D. Genome-wide linkage analysis and whole-exome sequencing identifies an ITGA 2B mutation in a family with thrombocytopenia. *Br. J. Haematol.* **2019**, *186*, 574–579. [[CrossRef](#)]
103. Kumar, V.; Gulzar, R.; Selvaraju, S.; Nazar, S.; Parthipan, S.; Prasad, R.V.; Jamuna, K.V.; Ravindra, J.P. Effect of bone morphogenetic protein-2 (BMP-2) on sheep granulosa cell steroidogenic function. *J. Cell Tissue Res.* **2014**, *14*, 4233–4236.
104. Lochab, A.K.; Extavour, C.G. Bone Morphogenetic Protein (BMP) signaling in animal reproductive system development and function. *Dev. Biol.* **2017**, *427*, 258–269. [[CrossRef](#)]
105. Tsai, H.L.; Chiu, W.T.; Fang, C.L.; Hwang, S.M.; Renshaw, P.F.; Lai, W.F.T. Different forms of tenascin-C with tenascin-R regulate neural differentiation in bone marrow-derived human mesenchymal stem cells. *Tissue Eng. Part A* **2014**, *20*, 1908–1921. [[CrossRef](#)] [[PubMed](#)]
106. Shahabi, A.; Tahmoorespour, M.; Kazemipour, A. Reconstruction, analysis and comparison of gene networks topology based on RNA-Seq data involved in reproductive and fertility complex traits. *Agric. Biotechnol. J.* **2019**, *11*, 57–78.

107. Demyanenko, G.P.; Mohan, V.; Zhang, X.; Brennaman, L.H.; Dharbal, K.E.; Tran, T.S.; Manis, P.B.; Maness, P.F. Neural cell adhesion molecule NrCAM regulates Semaphorin 3F-induced dendritic spine remodeling. *J. Neurosci.* **2014**, *34*, 11274–11287. [[CrossRef](#)] [[PubMed](#)]
108. Azumah, R.; Hummitzsch, K.; Hartanti, M.D.; St John, J.C.; Anderson, R.A.; Rodgers, R.J. Analysis of upstream regulators, networks and pathways associated with the expression patterns of polycystic ovary syndrome candidate genes during fetal ovary development. *Front. Genet.* **2021**, *12*, 2564. [[CrossRef](#)]
109. Slack, J.M. Metaplasia and transdifferentiation: From pure biology to the clinic. *Nat. Rev. Mol. Cell Biol.* **2007**, *8*, 369–378. [[CrossRef](#)]
110. Lu, D.; Chen, J.; Hai, T. The regulation of ATF3 gene expression by mitogen-activated protein kinases. *Biochem. J.* **2007**, *401*, 559–567. [[CrossRef](#)]
111. Gonzaga-Jauregui, C.; Gamble, C.N.; Yuan, B.; Penney, S.; Jhangiani, S.; Muzny, D.M.; Gibbs, R.A.; Lupski, J.R.; Hecht, J.T. Mutations in COL27A1 cause Steel syndrome and suggest a founder mutation effect in the Puerto Rican population. *Eur. J. Hum. Genet.* **2015**, *23*, 342–346. [[CrossRef](#)]
112. Yoshida, H.; Goedert, M. Phosphorylation of microtubule-associated protein tau by AMPK-related kinases. *J. Neurochem.* **2012**, *120*, 165–176. [[CrossRef](#)]
113. Imran, F.S.; Al-Thuwaini, T.M.; Al-Shuhaib, M.B.S.; Lepretre, F. A novel missense single nucleotide polymorphism in the GREM1 gene is highly associated with higher reproductive traits in Awassi sheep. *Biochem. Genet.* **2021**, *59*, 422–436. [[CrossRef](#)]
114. Wang, G.; Zhou, H.; Gong, H.; He, J.; Luo, Y.; Hickford, J.G.; Hu, J.; Wang, J.; Liu, X.; Li, S. Variation in the Lipin 1 Gene Is Associated with Birth Weight and Selected Carcass Traits in New Zealand Romney Sheep. *Animals* **2020**, *10*, 237. [[CrossRef](#)]
115. Wang, C.; Zhao, Y.; Yuan, Z.; Wu, Y.; Zhao, Z.; Wu, C.; Hou, J.; Zhang, M. Genome-Wide Identification of mRNAs, lncRNAs, and Proteins, and Their Relationship with Sheep Fecundity. *Front. Genet.* **2021**, *12*, 750947. [[CrossRef](#)] [[PubMed](#)]
116. Miao, X.; Luo, Q.; Zhao, H.; Qin, X. Ovarian transcriptomic study reveals the differential regulation of miRNAs and lncRNAs related to fecundity in different sheep. *Sci. Rep.* **2016**, *6*, 35299. [[CrossRef](#)] [[PubMed](#)]
117. Hernández-Montiel, W.; Collí-Dula, R.C.; Ramón-Ugalde, J.P.; Martínez-Núñez, M.A.; Zamora-Bustillos, R. RNA-seq transcriptome analysis in ovarian tissue of pelibuey breed to explore the regulation of prolificacy. *Genes* **2019**, *10*, 358. [[CrossRef](#)] [[PubMed](#)]